UNIVERSITY OF OXFORD

The role of serine metabolism in B lymphocytes

Amir Khan

Merton College

Word count: 13,824

Nuffield Department of Orthopaedics, Rheumatology and Musculoskeletal Sciences (NDORMS)

MSc (by Research) Molecular and Cellular Medicine

Trinity 2022

Supervisor: Dr Alexander Clarke

Co-supervisor: Prof Katja Simon

Acknowledgments

I would like to begin by thanking Dr Alex Clarke for providing me with the opportunity to do my MSc(Res) in his lab during an unexpected and uncertain time in September 2020.

Completing this thesis would not have been possible without the rest of the Clarke group – Eros Marin Millan, Matheswaran Kandasamy, Yavuz Yazicioglu and Julia Johnstone. I am grateful for the support, guidance and help you have all provided me with. I would like to give acknowledge to Yavuz for helping me with the mouse colonies and for the immunisation procedures for one of my experiments.

I would also like to thank other researchers from the Kennedy Institute that have helped me to continue persevering, by motivating and guiding me on many things I have required assistance with.

A very special thank you to all my close friends and family, especially my parents, that have supported and cheered me on through times of despair and joy during my time at Oxford.

Finally, I would like to thank Ula for being by my side, motivating and pushing me to do better and always brightening my day when things did not go as planned. The journey wouldn't have had been the same without you.

I am and will be forever grateful for all the invaluable experiences from my MSc, which has shaped me to become a stronger, independent scientist.

Table of Contents

List of Figures

List of Tables

Abbreviations

1C	One-carbon
3-PG	3-phosphoglycerate
3-PHP	3-phosphohydroxypyruvate
3-PS	3-phosphoserine
AID	Activation induced cytidine deaminase
ALDH	Aldehyde dehydrogenase
ATP	Adenosine triphosphate
ATF4	Activating transcription factor 4
ATR	Ataxia telangiectasia and rad3 related
BACH2	BTB Domain And CNC Homolog 2
BCL-xL	B cell lymphoma-extra large
BCL6	B cell lymphoma 6
BCR	B cell receptor
BIM	Bcl-2-like protein 11
BLIMP1	B lymphocyte induced maturation protein 1
C_H	Heavy gene constant region
CHEK1	Checkpoint kinase 1
CSR	Class switch recombination
CXCL12	C-X-C motif chemokine ligand 12
CXCL13	C-X-C motif chemokine ligand 13
CXCR4	C-X-C chemokine receptor type 4
CXCR5	C-X-C chemokine receptor type 5
DC	Dendritic cell
DSB	Double strand break

DZ	Dark zone
EBV	Epstein Barr virus
eIF2α	Eukaryotic translation initiation factor 2α
ERK	Extracellular signal-regulated kinase
Fab	Antigen binding fragment
Fc	Crystallizable fragment
FDC	Follicular dendritic cells
Fo	Follicular
FOXO1	Forkhead Box O1
GC	Germinal centre
GCN2	General control non-depressible 2
GLUT	Glucose transporter
GSH	Glutathione
GSK-3	Glycogen synthase kinase 3
HIF-1α	Hypoxia inducible factor 1-α
ICOS	Inducible T cell co-stimulator
ICOSL	ICOS ligand
Ig	Immunoglobulin
IL	Interleukin
IRF4	Interferon regulatory factor 4
ISR	Integrated stress response
LMP2A	Latent membrane protein 2A
LPS	Lipopolysaccharide
LZ	Light zone
MAPK	Mitogen-activated protein kinase

MAT	Methionine adenosyltransferase
MHC II	Major histocompatibility class 2
miRNA	MicroRNA
MMR	Mismatch repair machinery
mROS	Mitochondrial reactive oxygen species
MS	Methionine synthetase
MTHFD	Methyl tetrahydrofolate dehydrogenase
MTHFR	Methyl tetrahydrofolate reductase
mTORC1	Mammalian target of rapamycin complex 1
NEAA	Non-essential amino acids
NF-kB	Nuclear factor κ B
NOX	NADPH oxidase
NP-CGG	4-hydroxy-3-nitrophenyl acetyl–chicken γ-globulin
NRF2	Nuclear factor-erythroid factor 2-related factor 2
OPP	O-propargyl-puromycin
OXPHOS	Oxidative phosphorylation
PAMP	Pattern associated molecule pattern
PBS	Phosphate buffered saline
PHGDH	Phosphoglycerate dehydrogenase
PI3K	Phosphoinositide 3-kinase
PKC	Protein kinase C
PKCβ	Protein kinase C β
PKM2	Pyruvate kinase M2
PPP	Pentose phosphate pathway
PSAT1	Phosphoserine aminotransferase 1

PSPH	Phosphoserine phosphatase
PTM	Post translational modification
PVDF	Polyvinylidene difluoride
RB1	Retinoblastoma 1
ROS	Reactive oxygen species
S1PR1	Sphingosine-1-phosphate receptor type 1
SAH	S-adenosylhomocysteine
SAM	S-adenosylmethionine
SHM	Somatic hypermutation
SHMT	Serine hydroxymethyl transferase
SLE	Systemic lupus erythematosus
SLO	Secondary lymphoid organs
SRBC	Sheep red blood cells
SSP	Serine synthesis pathway
STAT6	Signal transducer and activator of transcription 6
TBMs	Tingible body macrophages
TBS	Tris buffered saline
TBS-T	Tris buffered saline with TWEEN® 20
TCA	Tricarboxylic acid
TCR	T cell receptor
Tfh	T follicular helper
Th	T helper
THF	Tetrahydrofolate
TLR	Toll-like receptors
TP53	Tumour protein p53

Treg	T regulatory cells
TYMS	Thymidylate synthetase
VHL	Von-Hippel Lindau
WT	Wild type
XBP1	X-box binding protein 1
αKG	α-ketoglutarate

Abstract

The serine synthesis pathway (SSP) has been identified as highly upregulated in metabolically active cells and feeds into 1C metabolism, helping to generate biosynthetic material for cell proliferation and cell survival. The SSP in the context of GC B cells has not been previously explored, and therefore, I sought to determine its role. I found no effect on proliferation or viability of serine and glycine deprivation on wild type B cells. I identified upregulation of the SSP during activation in replete media, which was further amplified when depriving B cells of serine and glycine. Immunoglobulin production is relatively decreased when stimulated B cells are cultured without serine. However, using B cell conditional phosphoglycerate dehydrogenase (PHGDH) knockout mice, following immunisation, there was a relative increase in IgG1+ GC B cells. When I activated and cultured B cells from Phgdh KO mouse in vitro, I also found a relative increase in IgG1+ B cells. Phgdh KO mouse B cells did not survive or proliferate without serine and glycine in vitro. Together, my findings indicate that the SSP, as well as serine and glycine availability, are involved in B cell proliferation and viability, as well as in the molecular control of immunoglobulin expression. These findings could help in understanding ways in which the SSP can be manipulated for clinical treatment of cancers and autoimmune disease.

Introduction

B cells and germinal centres

Germinal centres (GC) are structures which form in secondary lymphoid organs (SLO), namely, lymph nodes, the spleen, and Peyer's patches. They can also emerge at sites of chronic inflammation, as tertiary lymphoid structures. GCs are structures where B cells undergo immunoglobulin class switch recombination (CSR), as well as somatic hypermutation (SHM) of their immunoglobulin genes. This generates long-lived plasma cells, with high affinity and specificity for their target antigen, or memory B cells, for a rapid immune response when the antigen is reencountered.

B cell activation and the initiation of germinal centres

Within SLO, naïve $IgM^{+}IgD^{+}$ B cells organise with follicular dendritic cells (FDCs) to form B cell follicles, which are separated from the T-cell zone by the interfollicular region. Upon recognition of antigen, B cells migrate to the interfollicular region, where they interact with a specialised subset of CD4+ T cells, known as T follicular helper (Tfh) cells.

Tfh cells were first identified in tonsils and are found in B cell follicles of SLO, where they play a critical role in the GC reaction by providing co-stimulatory and cytokine signals (1–3). In the absence of Tfh cells, GCs do not develop (4). Tfh cells express the master transcriptional regulator B cell lymphoma 6 (BCL6) (5,6). Tfh cells differentiate from CD4+ T cells in a multistep process, primarily in the T cell zones of SLO, through dendritic cell (DC) priming (7). They further develop when interacting with B cells. Interactions between B and Tfh cells include through the T cell receptor (TCR) and major histocompatibility class 2 (MHC II)-peptide complexes expressed on

the surface of B cells (8). Costimulatory molecules, such as CD80 and CD86 (B7-1 and B7-2), are expressed on antigen-presenting B cells and interact with CD28 on Tfh cells (8). Another important co-stimulatory signal is through CD40/CD40L, a critical interaction required for the survival of B cells (8). B cells also provide inducible T cell co-stimulator ligand (ICOSL), which stimulates Tfh cells through ICOS **(9)**. ICOS-ICOSL is important for the maintenance for Tfh cells, and CD40 interactions with B cells cause a positive feedback loop to increase surface ICOS expression (10). These surface interactions between B and Tfh cells are crucial for GC development and maintenance.

B cells detect antigens using their B cell receptor (BCR) or ligands via toll like receptors (TLRs). BCRs consist of a plasma membrane-bound immunoglobulin molecule (Ig), and the signal transduction moieties, CD79a and CD79b (11). They can be activated in a T-independent or T-dependent manner. During T-independent activation, signal transduction is triggered by BCR cross-linking due to recognition of non-peptide repetitive epitopes and through B cell intrinsic pathways, such as through stimulation of TLRs (12). T-independent activation of B cells produces short term plasma cells, secreting low affinity IgM, the first antibody isotype secreted upon initial antigen recognition to help provide immediate immunity (13). This response typically occur as a result of strong signalling through TLRs expressed by B cells, which sense pathogen-associated molecular patterns (PAMPs) from viruses and bacteria, e.g. double stranded DNA (such as CpG), RNA, and lipopolysaccharide (LPS) (12). The majority of TLRs are endosomal, including those sensing DNA and RNA (14).

T-dependent activation of B cell results in activation through engulfment of cognate

antigen, leading to its degradation and presentation on the B cell surface in the form of peptide-MHC II complexes. These peptide-MHC complexes need to be presented to Tfh cells for B cells receive further activation and survival signals. Tfh cells express CD40L, which interacts with CD40 expressed on B cells and activates pathways required for proliferation and differentiation, such as the nuclear factor kappa B (NF-κB) and phosphoinositide 3-kinase (PI3K) pathways (15). NF-κB signalling is activated through the canonical and alternative pathways; the canonical pathway is activated by the BCR, TLRs and CD40, but the alternative pathway is activated by CD40 stimulation only (16). The NF-κB pathway regulates cell cycle progression through c-Rel, which acts to controls transcription factors involved in transcription of key cell-cycle regulators, e.g., MYC, IRF4 and E2F3-encoding genes (16). The PI3K pathway is important during B cell activation, as it allows for calcium mobilization, which is involved in the nuclear localization of NF-κB (17). The PI3K pathway is also involved in the initiation of mammalian target of rapamycin complex 1 (mTORC1) and Akt signalling pathways (17,18). mTORC1 integrates signals from the environment, such as nutrient stress, to control numerous cellular processes, such as cell growth, proliferation, metabolism, and protein translation. The main function of mTORC1 is to promote anabolism, by enhancing mRNA translation and upregulating proteins associated with ribosomes (19).

Two critical cytokines produced by Tfh cells are Interleukin (IL) 4 (IL-4) and IL-21. IL-4 maintains B cell survival through downregulation of pro-apoptotic proteins, such as Bcl-2-like protein 11 (BIM), which is induced by BCR stimulation (20). Upregulation of the anti-apoptotic transcription factor B cell lymphoma-extra-large (BCL-xL) is triggered in a signal transducer and activator of transcription 6 (STAT-6)-dependent

manner by IL-4 and BCR stimulation (21). IL-4 also exerts an anti-apoptotic function through induction of glycolysis, also through STAT-6 (22). IL-21 is a potent stimulator of B cell proliferation, apoptosis, immunoglobulin class switching, and differentiation of B cells to plasma cells, by inducing BCL-6 (23,24). IL-21 can also signal to Tfh cells in an autocrine manner, and induce expression of chemokine receptors required for T cell homing (25).

Not all B cells are destined for the GC reaction; some B cells move to the medullary cords to become short-term plasmablasts, producing low affinity antibodies towards the target antigen (26). This allows rapid production of antibodies during the early immune response. Additionally, some B cell may even become unswitched memory B cells (27). B cell clones compete for T signal and those with the highest affinity binding for antigen within the B cell pool will move to the middle of the follicle to undergo the GC reaction.

The germinal centre reaction

GCs are made up of distinct anatomical regions, known as the dark zone (DZ) and light zone (LZ). The DZ consists of densely packed and rapidly dividing B cells, termed centroblasts, and reticular cells expressing C-X-C motif chemokine ligand 12 (CXCL12) (28). The LZ consists of B cells, termed centrocytes, and is less densely packed, and also includes tingible body macrophages (TBMs), FDCs and Tfh cells (29). C-X-C chemokine receptor type 4 (CXCR4) is upregulated on centrocytes, allowing for movement towards the ligand, CXCL12, produced in the DZ (30). The highest expression of CXCL12 is in the DZ, forming a concentration gradient towards the LZ allowing movement between the two anatomical regions to occur. Once B cells

reach the DZ, they downregulate CXCR4. FDCs produce C-X-C motif chemokine ligand 13 (CXCL13), the ligand for C-X-C chemokine receptor type 5 (CXCR5) expressed on B cells. CXCL13 creates a concentration gradient which centroblasts can follow into the LZ from the DZ. Centroblasts can be identified as $CXCR4^{hi}CD83^{low}CD86^{low}$ and centrocytes as $CXCR4^{low}CD83^{hi}CD86^{hi}$ (32, 33). The cyclic expression of chemokine receptors between the DZ and LZ allows for the movement between the two anatomical regions.

Upon exiting the DZ, the BCRs that have undergone SHM and interact with antigens presented by FDCs in the light zone. If the antigen is recognised by the BCR, it is engulfed by the B cell and presented to Tfh cells through peptide-MHC II complexes (34). Interaction of B cells with Tfh cells promotes positive selection, for further SHM and proliferation in the DZ, or to leave the GC and become memory B cells or plasma cells. Cells that cannot bind antigen or have a low affinity, die by apoptosis due to neglect, as they fail to compete for Tfh survival and proliferation signals (34). TBMs are involved in the clearance of dead and dying cells.

Figure 1 highlights the germinal centre reaction in a schematic diagram.

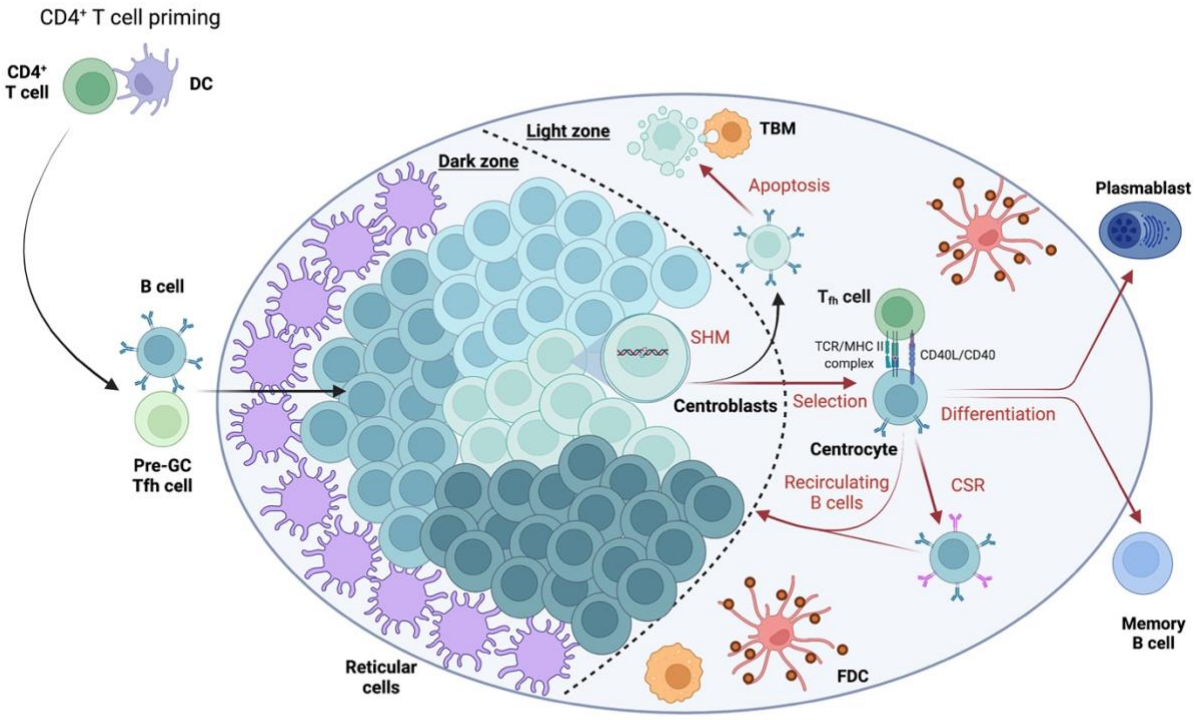

Figure 1 - The germinal centre reaction.
Tfh cells develop from CD4+ T cells after priming by DCs and upregulation of BCL6. B cells present antigen to Tfh cells, where they receive survival signals to move into the GC. Tfh cells gain further survival and development signals from B cells through co-stimulatory signals. B cells move into the DZ, where they undergo proliferation and SHM. The centroblasts move into the LZ, following a CXCL13 gradient produced by FDCs. Here, they interact with Tfh cells, and compete for their help. Centrocytes move into the DZ again, following a CXCL12 gradient produced by reticular cells, where they can further proliferate and undergo SHM of their immunoglobulin genes. Additionally, they can also undergo CSR before moving into the DZ. If no survival signals are received from Tfh cells, the centrocyte will die by neglect through apoptosis, where they are cleared up by TBMs. Created with BioRender.com

Class switch recombination and somatic hypermutation of immunoglobulin genes

Immunoglobulins, also known as antibodies in their secreted form, are made up of two heavy chain and two light chain molecules, formed in the shape of the letter “Y” (Figure 2). Immunoglobulins include antigen binding fragment (Fab) and crystallizable fragment (Fc) regions**.** Fab binds to the target antigen whilst Fc interacts with other immune cells or components, such as phagocytes or complement pathway components in secreted form (35). Immunoglobulins may undergo glycosylation, a posttranslational modification where a carbohydrate is added at specific sites, affecting the function of the antibody (35).

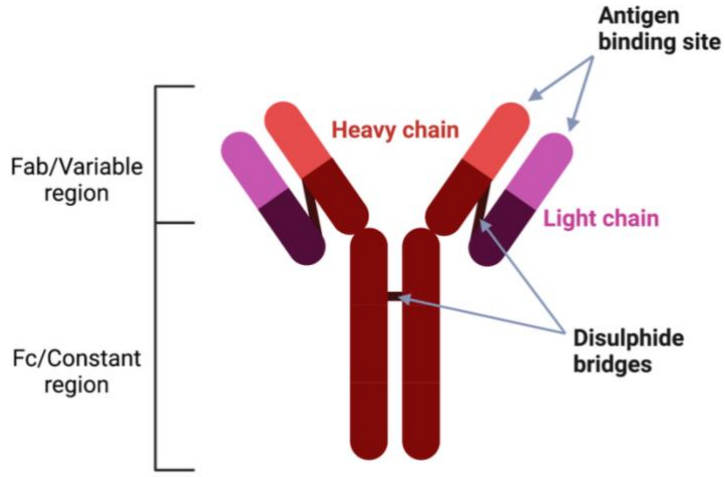

Figure 2 - Structure of an immunoglobulin molecule.
Immunoglobulins consist of two heavy (light and dark red) chains and two light chains (pink/purple), which are connected by disulphide bridges. The variable region, also known as the Fab, is the region where the antigen binds. The constant region, also known as Fc, is the region that undergoes CSR to other immunoglobulin subtypes. Created with BioRender.com

The mutagenic enzyme activation induced cytidine deaminase (AID) is responsible for

both CSR and SHM (36,37). AID is encoded by the *AICDA* gene and induces mutations by deaminating cytosine to uracil in DNA (38).

CSR is the process by which B cells change their gene encoding IgM towards the other isotopes; IgA, IgE or IgG. The heavy gene of the constant regions (C_H) is changed from the Cμ region, encoding IgM, to one of the other C_H genes, found in the order Cγ, Cε and Cα, giving rise to, respectively, IgG, IgE or IgA (39). Switch regions are present between the different C_H genes, starting from upstream of Cμ, which are excised to bring the downstream target constant region closer to the variable genes. Excision of the unwanted switch regions is repaired by double strand break (DSB) repair. Deleted DNA is removed in a extrachromosomal circular structure (39).

SHM is the process which results in random base insertion into the variable genes of the immunoglobulin locus at a high frequency (40). The activity of AID activates the error prone DNA mismatch repair (MMR) machinery, which cleaves the region where the mismatch occurred, leaving both strands of DNA exposed (39,41). Error prone DNA polymerases deposit random bases to bridge the gap produced by exonucleases (41). The addition of random bases in the immunoglobulin variable genes causes changes to the BCRs, which are then tested through Tfh interaction in the LZ. If selected, B cells are signalled to cycle through the DZ again to further allow mutation of their BCRs.

AID has an important role in both CSR and SMH and is error prone. It is therefore necessary to be able to regulate the expression, stability, and localization of AID. Two important ways to control AID epigenetically are through histone modifications and

miRNA expression. During activation of B cells, upregulation of enzymes involved in histone post translational modifications (PTMs) occurs, which alters gene expression through restricting or increasing access for transcription factors to target promoter sites. Activating PTMs are H3K4me3, H3K9ac and H3K14ac, whereas repressive PTMs are H3K27me3 and H3K9me3 (42) . MicroRNAs (miRNAs), such as mir-16, mir-155 and mir-181b, are also upregulated in response to repressive histone methylation markers, which then bind to complementary mRNA sequences of AID and therefore decreasing its expression (41,43). Phosphorylation has also been identified on AID protein at specific regions in activated B cells, which helps increase the activity of AID (44–46).

Regulators of the germinal centre reaction

BCL6 is the master regulator of GC B cell and Tfh cell differentiation. It is required for GC initiation (47). BCL6 deficiency results in decreased CXCR4, the chemokine receptor expressed on dark zone B cells (47). B cells deficient in BCL6 also show dysregulated sphingosine-1-phosphate receptor type 1 (S1PR1), which is expressed abundantly on B cells egressing germinal centres (48–50). BCL6 is also known to directly supress many DNA damage response genes, such as tumour protein p53 (TP53), ataxia telangiectasia and rad3 related (ATR) and checkpoint Kinase 1 (CHEK1), allowing tolerance for the DNA-damage response during SHM (51–53). BCL6 expression in Tfh cells upregulates the expression of CXCR5, which helps in localisation towards B cell follicles (2,3).

MYC is required by all proliferating cells, regulating numerous processes such as the cell cycle and metabolism. MYC is crucial in GC B cell precursor development, and its

deletion around day 2 post-immunisation results in failure to form GCs (54). MYC is also important in the LZ of the GC reaction and during later stages of the GC response (55).

B lymphocyte induced maturation protein 1 (BLIMP1) induces terminal differentiation of B cells into plasma cells (56). One way in which BLIMP1 induces plasma cell differentiation is through the downregulation of BCL6, extinguishing the GC gene expression program (57). Alongside gene downregulation, upregulation of plasma cell related genes occurs, such as X-box binding protein 1 (XBP1), the transcription factor involved in the production of the secretory machinery required for mass antibody production (57,58).

Forkhead Box O1 (FOXO1) plays a role in DZ B cell gene expression initiation and maintenance, and loss of FOXO1 has been shown to impair DZ formation (59,60). Since CXCR4 is one of the direct targets of FOXO1, it explains the defective DZ seen in FOXO1-deficient GC B cells (59,60).

BLIMP1 and BCL6 are reciprocally antagonistic transcription factors. BCL6 binds to the gene Prdm1 (which encodes BLIMP1), causing its repression (61). This inhibits the formation of plasma cells whilst allowing GC B cells to continue developing. BLIMP1 also directly represses BCL6 by binding to it (62).

Immune cell metabolism

General immune cell metabolism

Immune cells are amongst some of the most highly metabolically active cells in the body and are required to respond rapidly to environmental signals and following

receptor signalling. Immune cells use specific metabolic pathways during differentiation. An example is T cells; T helper (Th) cells (Th1, 2 and 17) are highly glycolytic, expressing high levels of GLUT1, whereas T regulatory (Treg) cells express less GLUT1 and have higher levels of fatty acid metabolism (63). The fate of T cells in becoming $\alpha\beta$ or $\gamma\delta$ lineage is also determined by metabolic cues. Activation of mTORC1 stops the production of reactive oxygen species (ROS), therefore promoting the $\alpha\beta$ T cell lineage but supressing commitment towards the $\gamma\delta$ T cell lineage (64). mTOR activation has also been shown to play a role in determining T lymphocyte fate. Following mTORC1 activation, CD4+ T cells differentiate towards Th cells, whilst differentiation towards Tregs and T cell anergy is inhibited, whereas CD8+ T cells adopt an effector fate (65).

Another example is DCs. DCs rely on aerobic glycolysis when activated, transitioning from their dependency on oxidative phosphorylation (OXPHOS) during their quiescent state. Blocking this switch to aerobic glycolysis has been shown to inhibit the maturation of DCs (66). Different subtypes of macrophages also display distinct metabolic preferences. Classically activated macrophages, also known as M1 macrophages, are proinflammatory, whereas alternatively activated macrophages, known as M2, are anti-inflammatory (67,68). M1 macrophages display increased glycolysis and pentose phosphate pathway (PPP) activity, but decreased OXPHOS (69–71). In addition, M2 macrophages are highly dependent on OXPHOS but reduce flux through the PPP (70–73). However, glycolysis has been found to be essential in M2 macrophages, although another study found glycolysis to be dispensable for their differentiation (74,75). This highlights the differential metabolic needs of immune cells to function in an inflammatory or anti-inflammatory manner.

Immune cells can also become pathogenic when metabolism becomes dysfunctional or dysregulated. A well-studied example is T cell metabolic dysregulation, which contributes towards systemic lupus erythematosus (SLE). Pathogenic CD4+ T cells have been found to have increased mitochondrial mass, ROS and reduced glutathione (GSH) (76). This leads to impaired activation-induced cell death but increased activation and necrosis, which contribute towards the activation of self-reactive lymphocytes (77). CD4+ T cells from lupus-prone mice and SLE patients, which have activated mTORC1, display increased glycolysis and decreased autophagy and mitophagy, which may contribute to the increased mitochondrial mass (78–80). DCs are also abnormal in SLE. DCs require mTORC1 for integrating numerous signals (81). With constitutive mTORC1 expression, their survival and proliferation is impaired, but their maturation was accelerated through MYC-mediated metabolic reprogramming, resulting in high ROS production (82).

Collectively, these examples highlight the diverse metabolism of different immune cell subsets, but also the complexity of targeting metabolism for treatment of disease.

B cell metabolism during activation and differentiation

Naïve peripheral B cells are metabolically quiescent cells and rely on fatty acid oxidation in order to maintain their long-term survival (83,84). Naïve B cells also have smaller mitochondrial mass, low glucose uptake and insensitivity to glycolysis inhibition, compared to activated B cells (84).

External stimuli trigger rapid changes in metabolism in B cells. Glucose uptake

increases in a PI3K-dependent manner following BCR stimulation (85). BCR stimulation also increases mitochondrial mass (83). B cells upregulate expression of Glucose transporter (GLUT) 1 (GLUT1) and GLUT3, correlating with increased glucose uptake (86). There is conflicting literature on how glucose is utilised by B cells during activation. Several studies have shown an increase in glucose uptake post-B cell activation, where inhibition of glycolysis resulted in shunting of glycolytic intermediates towards the PPP and impaired antibody production (83,85,87). However, Waters et al. also found glucose restriction did not affect activated B cell function, but rather activated B cells increase OXPHOS and sensitivity to OXPHOS inhibition and glutamine restriction increases (87).

The Protein Kinase C β isoform (PKCβ) is found to be abundant in B cells and is required for the increase in BCR induced glycolysis (88). Interrupting this pathway through loss of PKCβ has been demonstrated to disrupt mTORC1 activation, which in turn causes defective mitochondrial remodelling and metabolism and consequently, defective GC formation and plasma cell development (89).

Glucose can also be channelled towards the formation of lipids (87,90). Although B cells increase their metabolism and proliferation upon BCR stimulation, they require co-stimulation to avoid apoptosis through ROS accumulation and therefore mitochondrial dysfunction (91).

Epstein Barr virus (EBV) alters B cell metabolism to form B cell blasts, which enter germinal centres to generate memory B cells. Memory B cells act as reservoirs for EBV replication. EBV-induced latent membrane protein 2A (LMP2A) mimics BCR

signalling, leading to constant B cell activation and survival, and prevents lytic viral replication, through activation of PI3K and extracellular signal-regulated kinase (ERK)/mitogen-activated protein kinase (MAPK) (92–96). LMP2A is also involved in the uncoupling of BCR-dependent control of B cell tyrosine kinases, such as SYK and LYN, allowing for maintained activation (97). LMP2A interferes with cell-cycle checkpoints, such as P27, CHEK1 and retinoblastoma 1 (RB1), allowing continued proliferation, as well as interacting with MYC to inhibit proapoptotic effects (98). By hijacking and exploiting B cells, EBV can continue replicating and generating memory B cells, where it can stay latent. This demonstrates the importance of essential membrane proteins in initiating and controlling B cell expansion. EBV has also been implicated in altering one-carbon (1C) and mitochondrial metabolic pathways in infected B cells (99). By manipulating the 1C metabolism pathway to become upregulated, it provides antioxidants, methyl groups for epigenetic regulation, and DNA bases for proliferation.

Glycogen synthase kinase 3 (GSK-3) regulates metabolism during B cell maturation and maintenance, through phosphorylation of a wide range of proteins at serine or threonine residues (84). GSK-3 maintains naïve B cell survival through restricting the amount of cell mass accumulated, as well as being required for GC formation. Whilst maintaining B cell survival, it also regulates the amount of ROS produced and prevents apoptosis from occurring in glucose-limiting conditions (84).

It is evident that the stimulation of the BCR, CD40 or TLRs results in a rapid increase in ROS (100,101). ROS are required for B cell differentiation and their levels increase with activation and differentiation. Vene et al. demonstrated that inhibition of NADPH

oxidase (NOX) in B cells impairs activation and differentiation (102). Mitochondrial ROS (mROS) have also been demonstrated to play a role in B cell fate determination. Jang et al. showed a reduction in the synthesis of heme in B cells as a result of increased ROS causes an increase in CSR (103). Plasma cell differentiation was increased in B cells expressing more heme, causing BTB Domain And CNC Homolog 2 (BACH2) to be inhibited and BLIMP1 expression to be upregulated (103).

High levels of signalling through the PI3K/AKT/mTOR pathway inhibits FOXO1 and induces interferon regulatory factor 4 (IRF4) (104). IRF4, when transiently expressed in GC B cells, increases BCL6, whereas sustained expression of IRF4 represses BCL6, driving B cells towards the plasma cell lineage (105–107). FOXO1 is known to target P27, cyclin D2, the proapoptotic Fas-ligand, BIM, and ROS regulators, such as MnSOD (108). When B cells differentiate into plasma cells, production and secretion of antibodies occurs at a high rate, correlating with increased metabolic activity. BLIMP1 is thought to upregulate OXPHOS (109). Glucose taken up by plasma cells can be used for antibody glycosylation through the hexosamine pathway (110).

Together, this highlights the importance of metabolic reprogramming during B cell activation and in adaptation to cellular metabolic needs.

Germinal centre B cell metabolism

GC B cells have been shown to be sensitive to glycolysis inhibition, indicating its importance for survival and proliferation (84,111). On the other hand. fatty acid metabolism has been found to be used in preference to glycolysis in GC B cells (112). Through drug-induced and genetic inhibition of fatty acid oxidation, GC formation was

selectively reduced both in vivo and in vitro (112).

IL-4 signalling drives α-ketoglutarate (αKG) accumulation in B cells, resulting in epigenetic modification which upregulates BCL6, subsequently inducing GC B cell differentiation (87). Here, the development of GC B cells was found to be dependent on mitochondrial OXPHOS.

mTORC1 activity has been demonstrated to play a role in the formation of memory-prone B cells (113). A small population of GC-derived B cells with low mTORC1 activity contributed to both development and survival of B cells (113). This was also accompanied by increased BCL2 and surface BCR (113). mTORC1 has also been implicated in regulation of the DZ phenotype (114). Tfh signalling to B cells results in mTORC1 activation, which in turn promotes glucose uptake and cell growth. (114).

Transcriptional regulation also controls metabolism in GC B cells. c-MYC is found to be critical in GCs, directly upregulating expression of genes involved in glycolysis, uptake of nutrients and mitochondrial function, as well as glutaminolysis (115). c-MYC is upregulated in LZ B cells when Tfh cells signal through CD40 (116). The strength of selection signal received from Tfh cells determines the amount of c-MYC in the B cell (55). c-MYC is involved in regulating cell size, and acts as a timer controlling time in the DZ. MYC may act as an oncogene, driving GC B cell-derived lymphoma (55). The extent to which Tfh cells help B cells may be indicated in the metabolic capacity a B cell acquires before going through the cell cycle.

Hypoxia inducible factor 1-α (HIF1-α) stabilises in low oxygen tension, whereas Von

Hippel Lindau (VHL), destabilises HIF1-α in normal oxygen tension (117). LZs of GCs are thought to be hypoxic, resulting in HIF1-α stabilization. HIF1-α binds to and upregulates numerous genes, including those involved in glycolysis, but also causes reduced proliferation, increased GC B cell death, and impairs class switching by reducing expression of AID (118).

Together, these studies have demonstrated that multiple metabolic pathways and metabolic signals, both internal and external, are involved in the differentiation and proliferation of GC B cells. Epigenetic regulation is key for the development of B cells as well as determining GC B cell fates. Metabolites can help to enhance or repress gene expression, which may skew the development of B cells towards a particular subtype if there is an imbalance or preference of metabolic pathways.

One-carbon metabolism

1C metabolism is a process by which methyl groups are transferred through a cycle of three interlinked metabolic pathways: the de novo serine synthesis pathway (SSP), the folate cycle, and the methionine cycle. Together, these pathways are used to generate biosynthetic materials, such as amino acids and DNA bases, as well as contributing towards redox balance and epigenetic regulation, making it a crucial network in metabolically active cells (119).

The serine synthesis pathway

Serine is a non-essential amino acid (NEAA) which is utilised by cells in numerous cellular pathways, including 1C metabolism. Therefore, cells with a high proliferative capacity, such as malignant and activated immune cells, are often dependent on

serine from an external source to meet their metabolic demands (120,121). Serine is usually obtained from dietary sources, however, it can also be generated through the SSP as well as through catabolic mechanisms, such as autophagy (120).

Serine is an activator of the glycolytic enzyme, pyruvate kinase M2 (PKM2), which maintains the flux of intermediates through glycolysis (122). When the activity of PKM2 decreases, glycolytic intermediates upstream of this enzyme accumulate and thus 3-phosphoglycerate (3-PG) can enter the SSP (Figure 3). The first step of this pathway is the conversion of 3-PG to 3-phosphohydroxypyruvate (3-PHP) by the rate limiting enzyme phosphoglycerate dehydrogenase (PHGDH), in a NAD+ dependent manner (120). 3-PHP is then converted into 3-phosphoserine (3-PS) by phosphoserine aminotransferase 1 (PSAT1), in a glutamate dependent manner. αKG is generated as a result of glutamine being used by PSAT1. The final stage is the conversion of 3-PS to serine, catalysed by phosphoserine phosphatase (PSPH) (120).

SSP enzymes are upregulated when the integrated stress response (ISR) pathway senses stress, such as amino acid deprivation, through the GCN2-eIF2a-ATF4 axis (123). General control nonderepressible 2 (GCN2) binds to uncharged tRNA and when cells are deprived of amino acids (124). GCN2 phosphorylates eukaryotic translation initiation factor 2α (eIF2α), resulting in attenuation of global translation (125). eIF2α allows for protein synthesis to occur and its phosphorylation results in a cap-dependent translation block. However the translation of cap-independent proteins, such as activating transcription factor 4 (ATF4), is favoured, which can translocate to the nucleus to activate transcription of crucial genes for cell survival, as well as genes involved in helping to counteract the stressor (123).

Serine has also been found to contribute towards the activity of mTORC1 and long-term serine deprivation was found to repress mTORC1 (125). mTORC1 is actively involved in protein translation and its inhibition results in decreased protein synthesis (19). The GCN2- eIF2a-ATF4 axis is therefore important in upregulating the SSP, to help maintain serine levels during serine deprivation, which in turn maintains mTORC1 activity and sustains cell growth and proliferation.

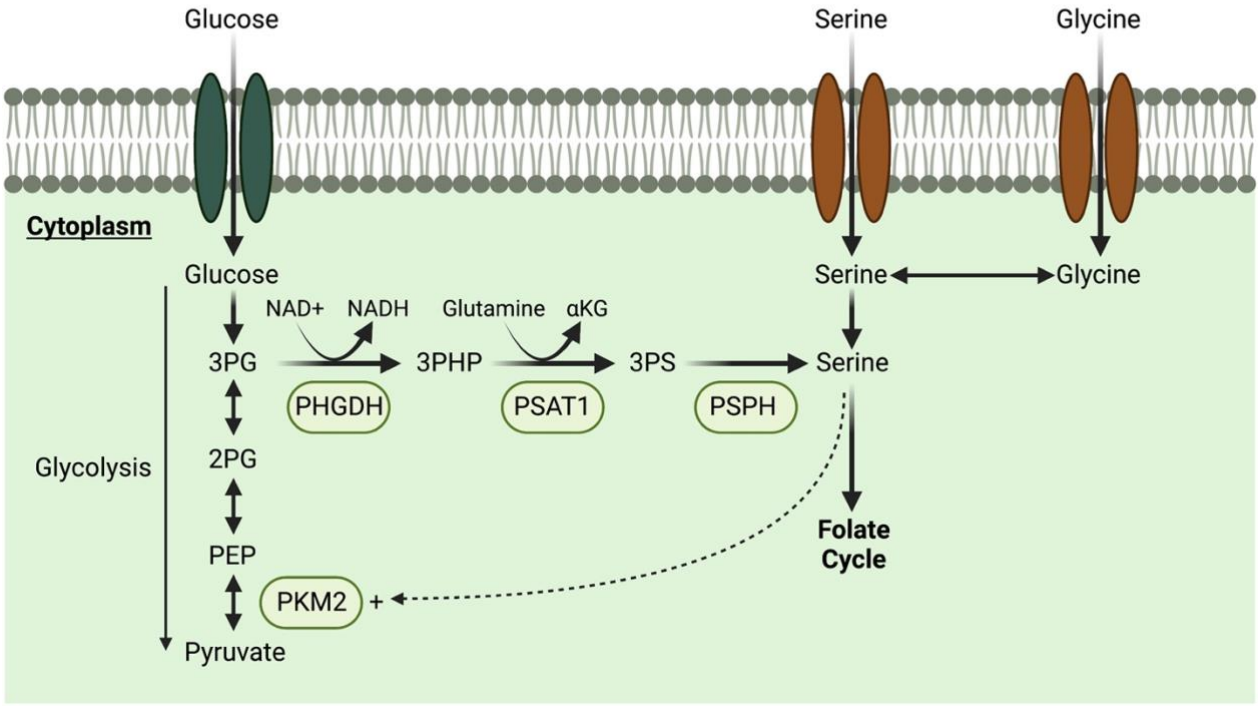

Figure 3 - The serine synthesis pathway.
Glucose is metabolised by glycolysis after being taken up by the cell through transporters. The glycolytic intermediate 3-PG can be used in the SSP, initially by the rate limiting enzyme PHGDH, which is NAD+ dependent. This forms 3-PHP, which is metabolised by PSAT1, a glutamine dependent enzyme, into 3-PS which is subsequently metabolised to serine by PSPH. Serine can be further metabolised in the 1C metabolism pathway. Serine can bind to PKM2 in an allosteric manner, causing its activity to be upregulated. During deprivation, the activity of PKM2 decreases, allowing for upstream intermediates to build up and therefore allowing to feed into the SSP. Created with BioRender.com. **This figure was inspired by Yang, M., Vousden, K. Serine and one-carbon metabolism in cancer. Nat Rev Cancer 16, 650–662 (2016).**

The folate cycle

The folate cycle supplies 1C units to other interlinked metabolic pathways, such as the methionine cycle and for the synthesis of glycine, NADH, nucleotide bases and GSH (120). The folate cycle takes place in both the cytosol and preferentially the mitochondria (126) (Figure 4).

The first step of the folate cycle converts tetrahydrofolate (THF) to 5,10-methylene-THF through the enzyme serine hydroxymethyl transferase 1/2 (SHMT1 is cytoplasmic and SHMT2 is mitochondrial) (120,127). 5,10-methylene-THF can be utilised for thymidylate synthesis through thymidylate synthetase (TYMS). It can also be used to produce 5-methyl-THF through methyl-tetrahydrofolate reductase (MTHFR), which contributes to the methionine cycle. Additionally, methyl THF dehydrogenase (MTHFD) catalyses the formation of 10-formyl THF. MTHFD1 is found in the cytoplasm and is NADP+ dependent. MTHFD2 (NAD+ dependent) and MTHFD2-like

(MTHFD2L) (NAD+ or NADP+ dependent) are mitochondrial enzymes catalysing the conversion. 10-formyl-THF can be used in numerous pathways e.g. for the synthesis of purines. Cytoplasmic aldehyde dehydrogenase 1 family member L1 (ALDH1L1) and mitochondrial ALDH1L2 catalyse the reaction for the regeneration of THF. Both enzymes are NADP+ dependent, helping to regenerate NADPH. Lastly, 10-formyl-THF can also be converted to formate, by cytosolic MTHFD1 and mitochondrial MTHFD1L in an adenosine triphosphate (ATP)-dependent manner (120,127).

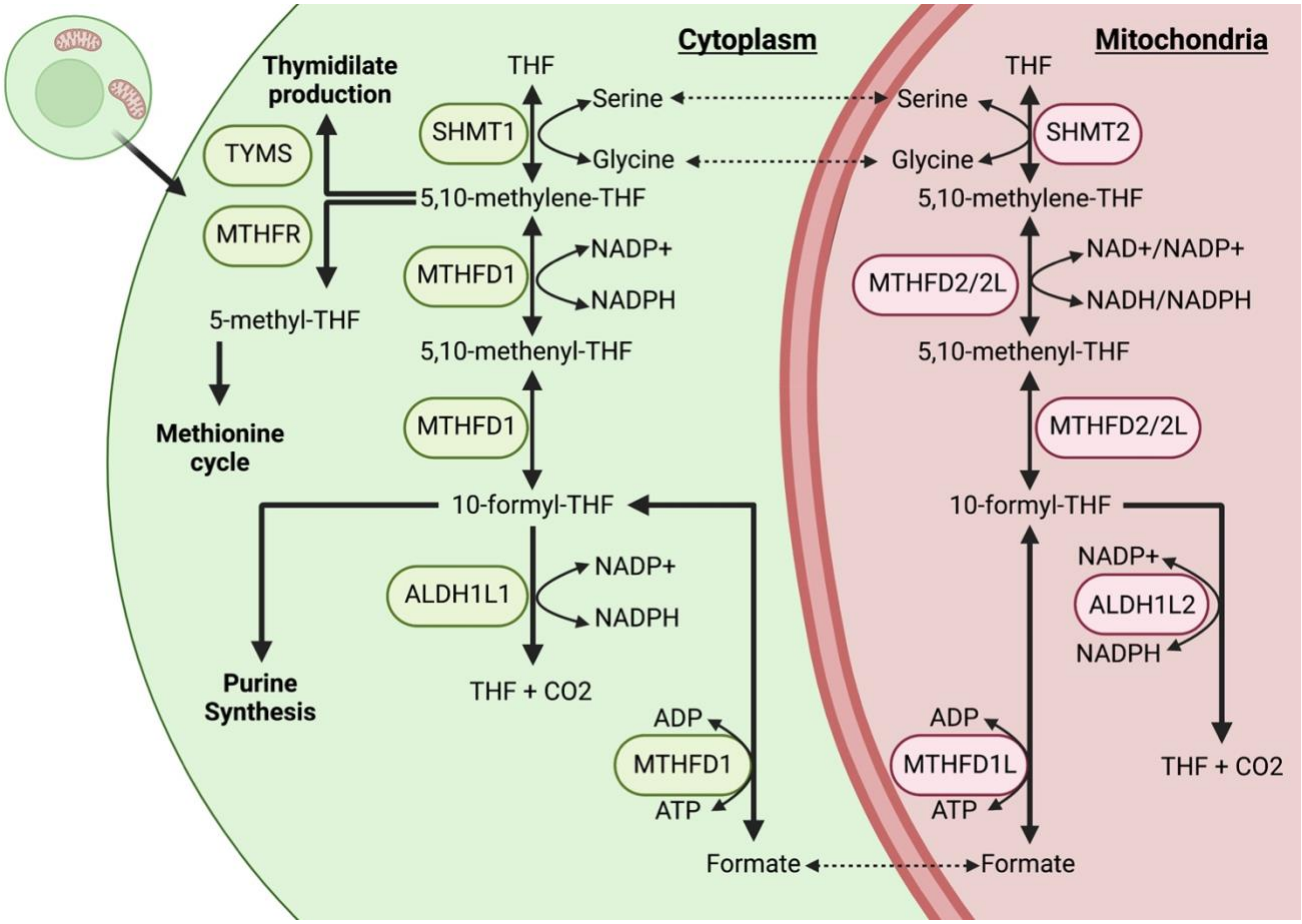

Figure 4 - The folate cycle

Serine is utilised by the folate cycle, with the first step being conversion into glycine through the enzymes SHMT1/2. Serine and glycine can move between the mitochondria and the cytoplasm. The conversion of serine to glycine allows for donation of a methyl group to THF to form 5,10-methylene-THF, which when formed in the cytoplasm, can also be used for thymidylate production, through TYMS, or for 5-methyl-THF production through MTHFR, contributing towards the methionine cycle. 5-10-meytylene-THF can be converted to 10-formyl-THF through MTHFD1 (cytoplasmic) or MTHFD2/2L (mitochondrial), in a NADP+ or NADP+ dependent manner. 10-formyl-THF, if formed in the cytoplasm can be used for purine synthesis. It can also be used to regenerate THF and produce CO2 in a NADP+ dependent manner both, by ALDH1L1 (cytoplasmic) or ALDH1L2 (mitochondrial). Additionally, it can also be converted to formate, through the enzymes MTHFD1 (cytoplasmic) and MTHFD1L (mitochondrial) in an ADP dependent manner, helping to regenerate ATP. Formate can move between mitochondria and the cytoplasm. The enzymes depicted in a green box are cytoplasmic, whereas those depicted in a red box are mitochondrial. Bidirectional arrows indicate the of the enzyme to work in a bidirectional manner. Created with BioRender.com. **This figure was inspired by Yang, M., Vousden, K. Serine and one-carbon metabolism in cancer. Nat Rev Cancer 16, 650–662 (2016).**

The methionine cycle

Methionine is an essential amino acid and is metabolised in a series of reactions. It is essential for the generation of the universal methyl donor, S-adenosylmethionine (SAM), involved in the methylation of nucleic acids, lipids, proteins and for epigenetic regulation (120,128). Methionine is generated from the donation of a methyl group from 5-methyl THF for homocysteine re-methylation through methionine synthetase (MS). Methionine is converted to SAM through methionine adenosyltransferase (MAT), which is an ATP-dependent process. Once SAM is used for methylation reactions, S-adenosylhomocysteine (SAH) is produced, which is then converted back to homocysteine, allowing for the cycle to continue again (120,128). Figure 5 shows a schematic diagram of the methionine cycle.

The transsulfuration pathway

The transsulfuration pathway branches off from the methionine cycle and is the route by which homocysteine is converted to cysteine, with the intermediate cystathionine (120). Homocysteine is generated in the methionine cycle from S-adenosyl-homocysteine. This pathway leads to the production of sulphur metabolites, such as the key antioxidant, GSH, as well as the production of the amino acid cysteine, and the signalling molecule hydrogen sulphide. Serine plays a role in this pathway too, in the conversion of homocysteine to cystathionine (120).

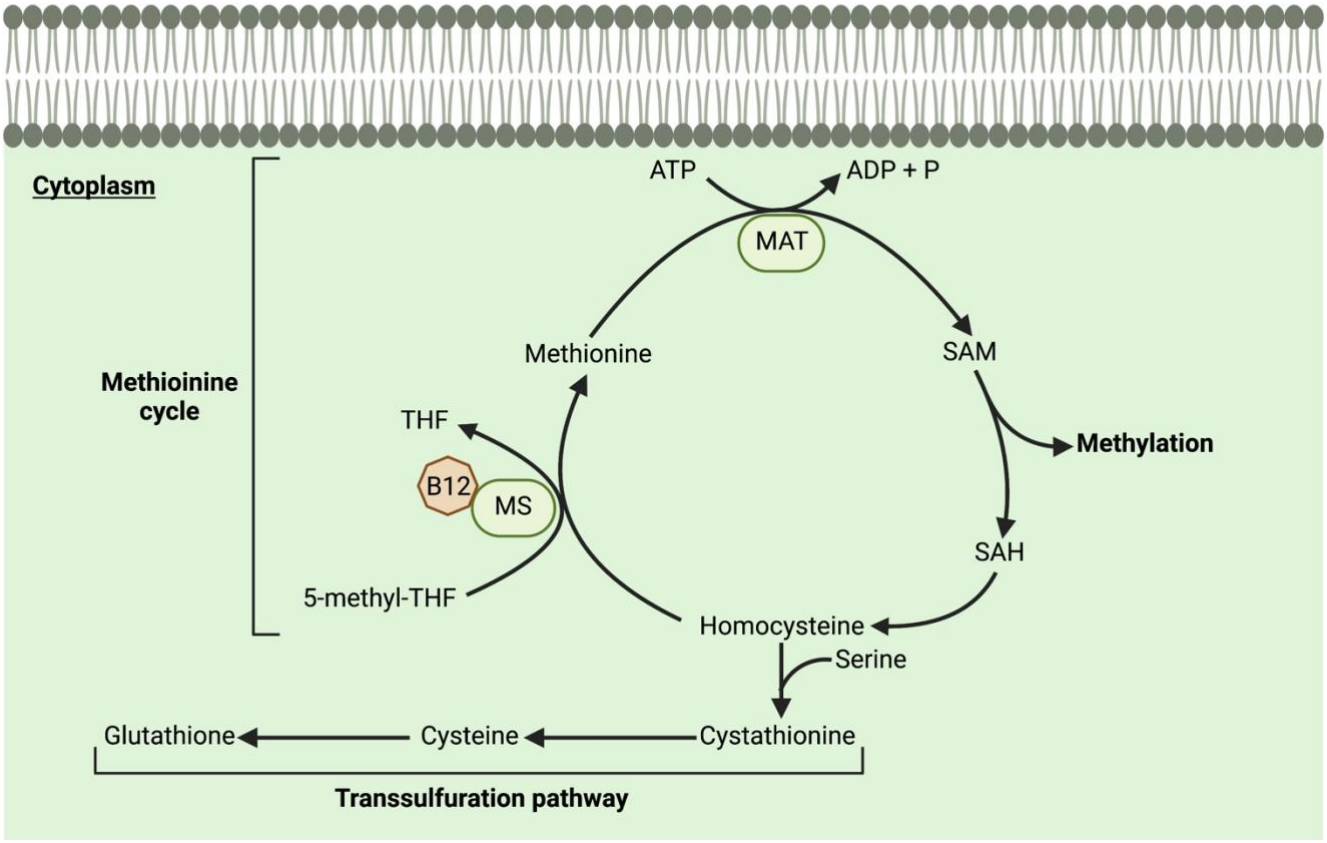

Figure 5 - The methionine cycle

5-methyl-THF from the folate cycle donates a methyl group to homocysteine to form methionine and THF. This step occurs through the enzyme, MS, which requires the co-factor, vitamin B12. Methionine is converted to SAM through MAT, in an ATP-dependent manner. SAM is used by the cell as a major methyl donor. Once the methyl group has been donated, SAH forms, which is converted back to homocysteine. Homocysteine can be cycled through the methionine cycle again or it can be shunted towards the transsulfuration pathway. In combination with serine, the intermediate cystathionine forms, which is converted to the amino acid cysteine. Cysteine can be used to synthetise the antioxidant, GSH. Created with BioRender.com. **This figure was inspired by Yang, M., Vousden, K. Serine and one-carbon metabolism in cancer. Nat Rev Cancer 16, 650–662 (2016).**

Significance of SSP and 1C metabolism in cancer and immune cells

Numerous cancer types overexpress the SSP as an adaptive response to extracellular nutrient starvation but also depend on extracellular consumption of serine for optimal growth (129–132). Overexpressing SSP enzymes may reduce the dependency of the tumour on extracellular serine, allowing growth in nutrient-deficient conditions.

Reduced PKM2 activity in tumours as a result of less activation by serine results in glycolytic intermediates feeding into the SSP (122). Since the flux of intermediates through the ATP generating step in glycolysis is reduced, it activates a stress response. To compensate for reduced ATP , OXPHOS is upregulated, which also provides ATP whilst increasing ROS (122). To dampen down the increased ROS, a compensatory increase in the PPP occurs, allowing for NADPH production (133).

In cancer cells, transcription factors are often dysregulated. c-MYC, one of the transcription factors which is overexpressed in many cancers, can induce the expression of PHGDH, PSAT1 and PSPH (134). Nuclear factor-erythroid factor 2-related factor 2 (NRF2) is another transcription factor abnormally expressed in cancers and which has also been found to increase SSP enzymes through ATF4 in non-small cell lung cancer, which helps to support the production of GSH and nucleotides (132). NRF2 also increases PPP enzymes, which are known to contribute to NADPH and nucleotide synthesis (135). Cancers expressing increased H3K9 methyltransferase G9A also display increased SSP. Serine deprivation results in mono-methylation at H3K9. Tumours depend on G9A for survival, although serine supplementation during G9A inhibition rescued the cancer cells (136). KDM4C removes the trimethylation from H3K9, a repressive marker for SSP genes and is required for ATF4-dependent

upregulation of the SSP (137). KDM4DC is also expressed abnormally in many cancers (138). Mitochondrial enzymes involved in 1C are upregulated in cancer cells. A tumour gene expression meta-analysis showed MTHFD2 to be consistently upregulated amongst numerous cancers. SHMT2 has been identified as upregulated and necessary for cancer cell growth (139). Together, these studies highlight the SSP and 1C enzymes to be of great importance in malignant states, especially when serine becomes limited.

Immune cells, both lymphocytes and myeloid, have also been shown critically require the SSP. 1C metabolism in T cells has been previously studied. T cells rapidly upregulate their 1C metabolism machinery upon activation (140). T effector cell proliferation was found to be impaired upon serine depletion, however the effector function of T cells was not affected (140). Ron-Harel et al. have demonstrated mitochondrial biogenesis and proteome remodelling during T cell activation (141). Inhibition of the mitochondrial 1C enzyme, SHMT2, results in impaired survival of CD4+ T cells in vitro and reduced the abundance of antigen-specific T cells in vivo (141). A later study, also conducted by Ron-Harel et al, showed T cells from aged mice have less activation of 1C metabolism and SSP compared to younger mice, as well as reduced metabolites of glycolysis, the tricarboxylic acid (TCA) cycle and PPP (142). T cells from aged mice also had smaller mitochondria, which may explain reduced metabolic activity. Interestingly, adding 1C metabolites rescued T cell activation in aged mice (142).

Rodriguez et al, have shown serine to be a requirement for GSH generation through the transsulfuration pathway in macrophages (143). GSH helps with the upregulation

of IL1β, a proinflammatory cytokine produced by macrophages, as well as contributing towards redox balance. Why macrophages require *de novo* serine produced intracellularly to increase IL-1β production remains unclear. One theory behind this may be to do with GSH helping to rescue macrophages from cell death (143). Furthermore, Yu et al., have shown methylation by SAM to play a role in pro-inflammatory macrophages, and SAM promotes the production of IL-1β (144). However, a study conducted by Kurita et al. showed serine depletion in LPS-stimulated macrophages to lead to less mitochondrial ROS and less activation of the SSP, but increased production of the inflammatory cytokine IL-6 (145).

1C metabolism in B cells has not been extensively studied. A study conducted by Wang et al. investigated changes in B cell metabolism post-EBV infection (99). They identified the SSP and 1C metabolism enzymes, particularly MTHFD2, to be activated early during infection by MYC and the viral protein, EBNA2, rather than by ATF4 specifically. Replacing glucose with galactose in culture media impaired the proliferation of infected B cells, indicating the importance of glycolysis during EBV-infected B cell growth. 1C metabolism feeds into GSH, nucleotide, NADPH and ATP synthesis, and therefore may aid infected B cells in sustaining proliferation and counteracting ROS (99). Very recently, D'Avola et al. published a paper investigating the SSP in GC B cells (146). They have also shown GC formation impairment post-immunisation in B-cells with a conditional PHGDH deletion. They injected mice with a pharmacological PHGDH inhibitor before immunising with 4-hydroxy-3-nitrophenyl acetyl–chicken γ-globulin (NP-CGG), which led to decreased IgG1 NP-specific plasma cells and serum anti-NP IgG1 but no difference in NP-specific IgM plasma cells or anti-NP IgM. This study indicates the importance of PHGDH in GC formation, as well as in

immunoglobulin class switching (146).

Together, these studies have demonstrated that serine is required by highly proliferative cells, both in pathological and normal states, for survival and proliferation. When serine is limited, the SSP is upregulated as a compensatory mechanism.

Aims and hypothesis

Aims

This aims of my thesis are to:

1. Determine the effects of serine and glycine deprivation on B cells.
2. Determine the effects of B cell specific Phgdh deletion in vivo, using Mb1-cre Phgdh-flox mice.

Hypothesis

The hypothesis of this project is "***B cell activation and differentiation increases as flux through 1C metabolism increases***".

Methods and materials

Mice

Mb1-cre Phgdh-flox mice (147,148) aged 6-15 weeks were euthanised in a CO_2 chamber, with confirmation of death by cervical dislocation. An incision was made in the upper left abdomen, and spleens were extracted and placed in 1.5ml microcentrifuge tubes containing 500μl of complete RPMI-1640. These mice were maintained at the animal facilities in specific pathogen-free conditions, at the Kennedy Institute of Rheumatology, University of Oxford. All procedures were carried out under project licence from the UK Home Office.

Splenic B cell isolation

Freshly isolated spleens were injected with FACS buffer (1x PBS with 0.5% BSA and 2mM EDTA), before being crushed through a 70 μm nylon cell strainer. The cell suspension was washed with FACS buffer and then centrifuged at 400g, 4ºC for 5 minutes. B cell isolation was carried out using mouse Pan B Cell Isolation Kit II (Miltenyi Biotec), The pellet was resuspended in 100μl FACS buffer and incubated with 25μl Fc Receptor Blocking Reagent and 50μl Pan B Cell Biotin-Antibody Cocktail and incubated at 4ºC for 5 minutes. After incubation, the cells were diluted in 150μl FACs buffer and incubated with 100μl Anti-Biotin MicroBeads at 4ºC for 10 minutes. Post-incubation, B cells were filtered through a 70 μm pre-separation filter (Miltenyi Biotec) and separated with an LS column (Miltenyi Biotec). Cells were counted using trypan blue and Countess™ Cell Counting Chamber Slides (Invitrogen) on the EVE™ Automatic Cell Counter (NanoEnTek) after isolation. Proliferation was measured by incubating with CellTrace™ Violet (CTV) Cell Proliferation Kit (Invitrogen) at a dilution

of 1:2000. Cells were incubated at 37ºC for 15 minutes before washing with FACS buffer and centrifuging. The pellet was resuspended in FACS buffer and cells were counted again. Isolated B cells were placed on ice until ready to be plated.

Cell culture medium

Serine- and glycine-free RPMI-1640 (Teknova) was supplemented with 10mM glucose, 2mM GlutaMAX, 1mM pyruvate, 10mM HEPES, 100 IU/ml Penicillin/Streptomycin and 50μM 2-mercaptoethanol. 10% dialysed FBS was added to the media. Powdered serine (Sigma) and glycine (Sigma) were diluted in miliQ water and added to wells at a final concentration of 30mg/L and 10mg/L. Cells were cultured in 96-well round bottom for flow cytometry, ELISA and qPCR analysis or 48-well flat bottom plates for western blotting analysis. All experiments were carried out in a cell culture hood, in sterile conditions. The table below highlights the mix of stimulants used for B cells and the number of cells plated throughout this thesis.

Table 1 - Stimulation mixes used for B cell activation and number of

cells plated.

Stimulation mix	Number of cells plated per well
10mg/ml Anti-CD40 agonistic antibody (Clone: FGK45.5) (Miltenyi Biotec) and 1ng/ml recombinant murine IL-4 (Peprotech)	- 200,000 cells for flow cytometry experiments. - 200,000 cells plated for OPP uptake experiment
10mg/ml anti-CD40 agonistic antibody (Clone: FGK45.5) (Miltenyi Biotec) and 0.1mM ODN1826 (Class B CpG) (Miltenyi Biotec)	- 200,000 cells plated for flow cytometry experiments. - 1.5 million cells plated for western blotting
1ug/ml anti-CD40 agonistic antibody (Clone: FGK45.5) (Miltenyi Biotec), 25ng/ml recombinant murine IL-4 (Peprotech), 10ng/ml recombinant murine IL-21(Peprotech) and 10ug/ml LPS, E. Coli O111:B4 (Merck)	- 100,000 cells plated for flow cytometry experiments.

Western blotting

Cells obtained from cell cultures were washed with 10ml of cold Phosphate Buffered Saline (PBS) for 10 minutes at 450g, 4ºC for 5 minutes. Cells were lysed using 100µl RIPA buffer (ThermoFisher) containing cOmplete™ ULTRA Mini Protease Inhibitor (Roche) and PhosSTOP™ (Roche) for 15 minutes on ice, with regular vortexing. The samples were microcentrifuged at 17,000g for 5 minutes at 4ºC. The supernatant was collected into another 1.5ml microcentrifuge tube and stored at -20ºC. Protein quantification was carried out using the Pierce™ BCA Protein Assay Kit (Thermo Scientific). For protein quantification, samples were diluted 10 times in miliQ water and were added in duplicate wells in a 96-well plate. For protein denaturation, 4X Laemmli sample buffer (Biorad) mixed with 5% 2-mercaptoethanol (Sigma) was added to the

15μg of sample lysate, which was then placed in a heating block at 95ºC for 5 minutes and then immediately transferred to ice. The sample mix was then pipetted into the wells of 4–20% Mini-PROTEAN® TGX™ Precast Protein Gels (Biorad) and ran, before transferring to a polyvinylidene difluoride (PVDF) membrane using the Trans-Blot Turbo Transfer System (Biorad). The PVDF membrane was stained with Ponceau S stain to confirm transfer onto the membrane. The membrane was then dried for 1 hour before blocking with 5% full-fat milk in Tris-Buffered Saline (TBS) with 0.05% TWEEN® 20 (TBS-T) at room temperature, for 1 hour. The membrane was then incubated with primary antibodies at the indicated dilutions overnight at 4ºC. Primary antibodies were diluted accordingly to manufacturers protocol in 2.5% skimmed milk powder or 2.5% BSA in TBS-T. After the incubation, the membrane was then submerged and washed once with TBS-T for 5 minutes to remove unbound primary antibody, before incubation with a secondary antibody in 2.5% milk in TBS with 0.01% SDS at room temperature. The blot was then washed 3 times for 5 minutes in TBS-T. The membrane was then placed in TBS to prevent it from drying. The membrane was analysed using the Li-COR Odyssey imaging machine. Primary and secondary antibodies used for western blotting are mentioned in the table below.

Table 2 - Antibodies used for western blotting.

Antibody specificity	Species	Manufacturer	Dilution

Anti-vinculin (E1E9V)	Rabbit	Cell signalling	1:2000
Anti-alpha Tubulin (DM1A)	Mouse	Cell signalling	1:2000
Anti-PHGDH	Rabbit	Cell signalling	1:2000
Anti-PSAT1	Rabbit	Cell signalling	1:2000
Anti-Histone H3 (D1H2) XP®	Rabbit	Cell signalling	1:2000
Anti-H3K4Me3 (C42D8)	Rabbit	Cell signalling	1:1000
Anti-mouse IgG (H+L)	Alexa Fluor™ 790 Donkey	Invitrogen	1:20,000
Anti-rabbit IgG (H+L)	Alexa Fluor® 680 Goat	Invitrogen	10x less than the primary antibody

Flow cytometry

Cells were plated in a conical V-bottom plate and centrifuged at 450g for 5 minutes at 4ºC. The supernatant was discarded, and the pellets were incubated with 100μl of eBioscience™ Fixable Viability Dye eFluor™ 780 (Invitrogen) at a dilution of 1:1000 in PBS for 20 minutes on ice. The wells were washed with PBS and centrifuged at 400g for 5 minutes at 4ºC. The supernatant was discarded and cells were incubated with CD16/CD32 Fc block diluted in PBS for 10 minutes, before washing with PBS. The supernatant was discarded and cells were incubated with 50μl of antibody cocktail mix for 30 minutes on ice. The pellets were washed with PBS and centrifuged at 400g for 5 minutes at 4ºC. If cells were not to be fixed, the pellet was then resuspended in 200μl of FACS buffer and placed into cluster tubes. If cells were fixed, the pellets were resuspended in 100μl of Intracellular Fixation Buffer (eBioscience™) for 45 minutes. The cells were washed three times with 100μl PBS and centrifuged at 400g for 5 minutes at 4ºC, and the supernatant was discarded. The pellet was resuspended in 200μl FACs buffer and placed into cluster tubes. Data was generated on BD® LSR II or BD LSR Fortessa™ flow cytometers. Data was analysed using the FlowJo™ 10 software.

Table 3 - Antibodies used for flow cytometry

Antibody specificity and fluorochrome	Type	Clone	Dilution	Manufacturer
Anti-CD19 PE	Mouse	REAffinity™ REA749	1:200	Miltenyi Biotec
Anti-CD19 BV510	Mouse	6D5	1:200	Biolegend
Anti-B220 BV510	Mouse	RA3-6B2	1:200	Biolegend
Anti-IgG1 PerCP Cy5.5	Mouse	RMG1-1	1:50	Biolegend
Anti-CD138 PE	Mouse	281-2	1:75	Biolegend
Anti-CD86 BV421	Mouse	GL-1	1:100	Biolegend
Anti-CXCR4 PE	Mouse	I.276F12	1:40	Miltenyi Biotec
Anti-IgM PE-Cy7	Mouse	RMM-1	1:200	Biolegend
Anti-IgD BV650	Mouse	11-26c.2a	1:400	Biolegend
Anti-CD16/32 (Fc Block)	Mouse	2.4G2	1:200	BD
Anti-GL7 AF647	Mouse	GL7	1:75	Biolegend
Anit-TACI PE	Mouse	8F10	1:250	Biolegend
Anti-Gr1 APC Cy7	Mouse	RB6-8C5	1:100	Biolegend
Anti-GL7 Alexa Fluor 488	Mouse	GL7	1:75	Biolegend
CellTrace™ Violet Cell Proliferation Kit	Mouse	-	1:1000	Invitrogen

IgM ELISA quantification

Mouse IgM ELISA was carried on cell culture medium from experiments carried out over 3, 4 and 6 days, following manufacturer's instructions (Invitrogen). Supernatant was collected and cells were counted. Wash buffer was made using 0.05% Tween-20 in 1X PBS. A flat bottom high-affinity protein binding 96 well plate (Corning) was incubated overnight at 4ºC with capture antibody at a 1:250 dilution in coating buffer (1X PBS). The plate was then washed twice with wash buffer the subsequent day and blotted on absorbent paper to remove residual buffer from wells. The plate was then blocked with blocking buffer (2X Assay Buffer A) overnight at 4ºC. The following day, the plate was washed twice with wash buffer and blotted dry. The standards provided were reconstituted in deionised water and a 2-fold serial dilution in duplicates was made. Samples were diluted in 1X Assay Buffer A at a dilution of 1:50, before being plated in the wells at the required volumes. The plate was washed 4 times in wash buffer and blotted dry, before the IgM detection antibody was added for 1 hour incubation at room temperature. The plate was then washed again 4 times, after the 1-hour incubation with wash buffer. The detection antibody was diluted 1:250 in 1X Assay Buffer A. After the detection antibody incubation, TMB substrate solution was added to the plate and incubated at room temperature for 15 minutes, before adding stop solution (2N sulfuric acid) to the wells. Analysis was carried out using the FLUOstar Omega (BMG LABTECH).

RNA extraction, cDNA conversion and RT-qPCR

RNA extraction was carried out using the RNeasy mini kit (QIAGEN), following manufacturers protocol. Upon RNA isolation, RNA concentration and purity was measured using the NanoDrop™ One Spectrophotometer (Thermofisher). RNA was converted to cDNA using the High-Capacity RNA-to-cDNA™ Kit (Applied Biosystems), following manufacturers protocol. cDNA was diluted with 180μl RNAse-free water to dilute the sample 10 times. Samples were stored in a -20ºC freezer for storage. qPCR was carried out using 0.5μl TaqMan probe (Thermofisher), 5μl TaqMan™ Fast Advanced Master Mix (Applied Biosystems), 1μl cDNA and 3.5μl RNAse free water in a 384-well V-bottom plate. The plate was placed in the ViiA™ 7 Real-Time PCR System (Thermofisher) to undergo 40 cycles. Using the delta-CT method, all values are normalised to *Ubc*. Ser/Gly deprived condition values were calculated relative to the Ser/Gly fed control wells, due to intra-experimental variation. TaqMan primers used for qPCR are listed in the table below.

Table 4 - Table of TaqMan primers used for qPCR

Primer	**Reference**
Ubc	Mm01198158_m1
Ptprc	Mm01293577_m1
Phgdh	Mm01623589_g1
Psat1	Mm04932904_m1
Aicda	Mm00507774_m1
Slc2a1(Glut1)	Mm00441480_m1

In vivo immunisation and analysis

Mb1-cre Phgdh-flox Mice aged 9-12 weeks were immunised with 200μl Sheep red blood cells (SRBC). 1ml sterile SRBC (ThermoFisher), which was washed with 15ml cold PBS twice, before reconstituting in 3ml PBS. Sterile SRBC was administered as 0.2ml intraperitoneal injections to the mice. Mice were culled at day 9 and the spleens were harvested. The spleens were split in half; one half was used for preserving the sample for microscopy and the other half for flow cytometry analysis. The half spleens were crushed on a 70μm cell strainer, before washing with PBS at 400g 4ºC for 5 minutes. The supernatant was discarded, and the pellet was disrupted with 3ml of red blood cell lysis buffer (Gibco) for 3 minutes, before being washed with PBS at 400g, 4ºC for 5 minutes. Cells were counted and 2 million cells were plated in each well of a 96-well conical V-bottom plate. The plate was centrifuged at 400g 4ºC for 5 minutes. Cells were incubated with Fixable Viability Dye eFluor™ 780 (eBioscience™) for 20 minutes on ice. The cells were wash with PBS, before discarding the supernatant. The pellets were then incubated with 50μl Fc block antibody for 5 minutes, before adding 50μl of a 2X antibody mix for 30 mins. The cells were washed with FACS buffer and resuspended in FACs buffer, before being transferred to cluster tubes for running on the BD LSR Fortessa™ flow cytometer.

Click-iT™ OPP reaction

OPP uptake was carried out using the Click-iT™ Plus OPP Alexa Fluor™ 647 Protein Synthesis Assay Kit (Invitrogen™). Cells were washed with PBS at 400g 4ºC for 5 minutes. The cells were incubated with 100μl Click-iT® OPP Reagent (Component A) in a 1:1000 dilution in complete culture medium for 30 minutes in an incubator at 37ºC, 5% CO_2. Cells were centrifuged at 400g, 4ºC for 5 minutes, before washing once with cold PBS. Cells were then incubated with CTV and antibodies and fixed, according to the *Flow cytometry* protocol. After fixation, the cells were then washed with 1X permeabilization buffer at 400g for 5 minutes (eBioscience™). Cells were incubated with 1X permeabilization buffer and the pellet for 30 minutes at room temperature. Cells were then washed with PBS at 400g, 4ºC for 5 minutes. The Click-iT reaction was carried out using the reaction cocktail consisting of copper protectant (Component D), fluorochrome-conjugated picolyl azide (component E), 1X reaction buffer additive in 1X reaction buffer. The cells were resuspended in 100μl of the reaction cocktail and incubated at room temperature in the dark for 30 minutes. The cells were washed once with 100μl Click-iT® reaction rinse buffer (Component F). The cells were then resuspended in 200μl FACS buffer and placed in cluster tubes for analysis on the BD LSR Fortessa™ flow cytometer.

Results

1 – The importance of serine and glycine during B cell activation and proliferation

1.1 – Exogenous serine and glycine are dispensable for B cell proliferation and viability

I initially sought to determine how proliferation and viability of B cells is affected by serine and glycine deprivation. B cells were isolated from wild type (WT) mouse spleens and incubated with CTV proliferation tracking dye. They were then stimulated with anti-CD40 agonistic antibody and IL-4 (Figure 6A). The anti-CD40 agonistic antibody works by stimulating B cells through the CD40 receptor, which triggers NF-κB signalling, promoting B cell survival and proliferation (16). IL-4 stimulates the IL-4R on B cells, promoting B cell survival (20). B cells were cultured either with serine and glycine, without serine and glycine, with serine only or with glycine only, for 72 hours. Cell culture media used is serine and glycine deplete, therefore supplementation was required. Serine and glycine were diluted in deionised water and added to wells at a concentration of 30mg/L and 10mg/L. These four conditions were used to determine if the presence of one or the other amino acid had an impact on cell viability or proliferation. Cells were cultured without serine and glycine, since interconversion between serine and glycine can occur. Flow cytometry was then carried out on these cells, using an antibody for the B cell surface marker, CD19, and viability dye to gate live B cells (Figure 6B). Depleting serine or glycine did not affect cell viability or cell division (Figure 6C, D and E).

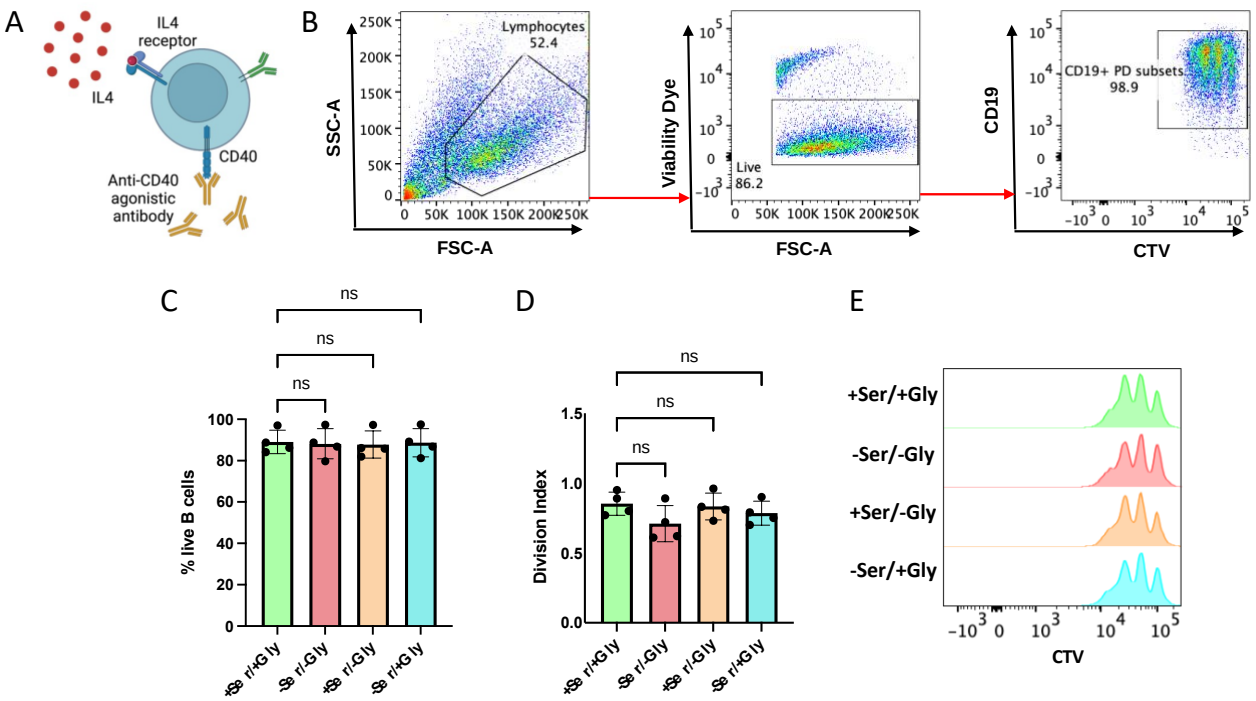

Figure 6 – Serine and glycine deprivation does not affect B cell division or viability when stimulated through IL-4R and CD40.

A) Schematic of recombinant murine IL-4 and anti-CD40 stimulation used to activate splenic B cells over 72 hours (Created with BioRender.com). B) Representative gating strategy of live CD19+ B cells. C) B cell viability graph of cells cultured in different serine/glycine conditions. D) Division index of B cells in different serine/glycine conditions. E) Representative CTV proliferation histograms of splenic B cells cultured in different conditions with serine/glycine. B and C are n=4, with 2 biological replicates from 2 independent experiments. Statistical analysis was carried out using one-way ANOVA. For statistical analysis, non-significance (ns) = P ≥ 0.05.

To test whether this was an IL-4-specific response to serine/glycine deprivation, I cultured cells in the same conditions, but stimulated with ODN1826 and anti-CD40 agonistic antibody instead. ODN1826 is a short sequence of single stranded DNA, consisting of CpG motifs, which acts through TLR9 (12) (Figure 7A). Flow cytometry was carried out on these cells, using an antibody for CD19 and viability dye to gate live B cells (Figure 7B). Again, I found no significant difference in viability or cell division (Figure 7C, D and E). No difference in cell viability or division was identified when an alternative B cell stimulant was used, indicating an underlying mechanism by which viability and division is maintained during serine and glycine deprivation.

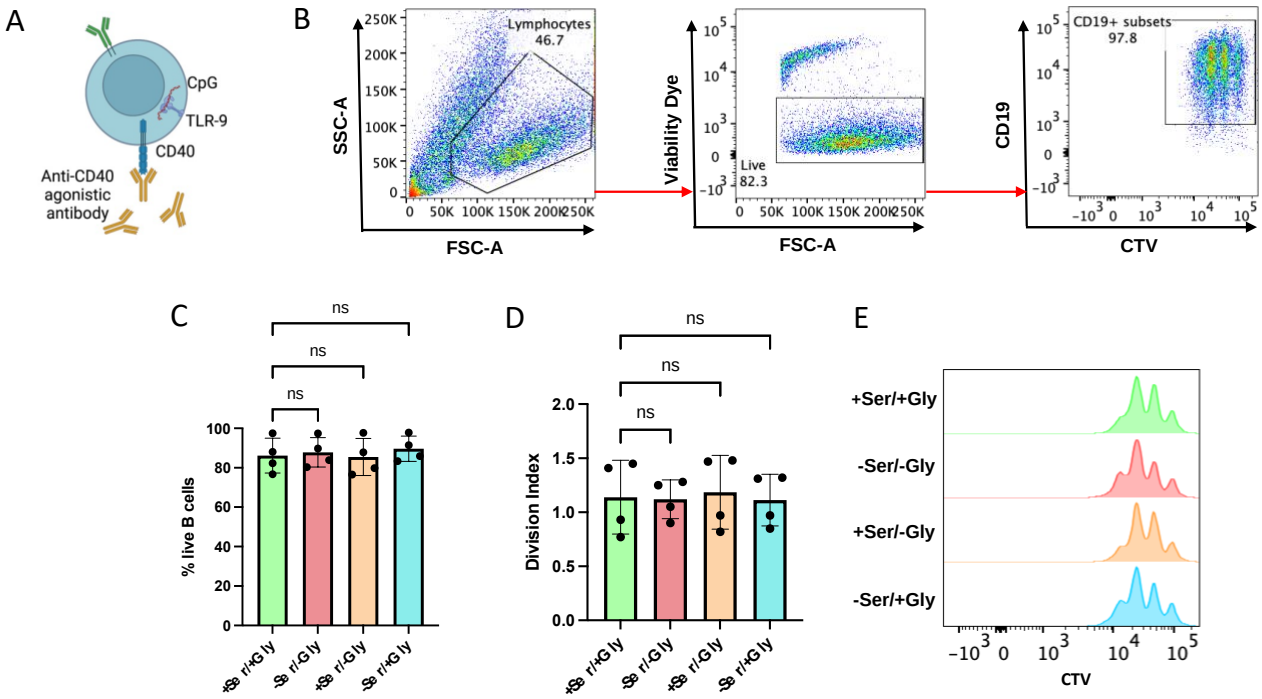

Figure 7 - Serine and glycine deprivation does not affect B cell division or viability when stimulated through TLR9 and CD40.

A) Schematic of ODN1826 and anti-CD40 stimulation used to activate B cells over 72 hours (Created with BioRender.com). B) Representative gating strategy of live CD19+ B cells. C) B cell viability graph of cells cultured in different serine/glycine conditions. D) Division index of B cells in different serine/glycine conditions. E) Representative CTV proliferation histograms of splenic B cells cultured in different serine/glycine conditions. B and C are n=4, with 2 biological replicates from 2 independent experiments. Statistical analysis was carried out using one-way ANOVA. For statistical analysis, non-significance (ns) = $P \geq 0.05$.

1.2 – Expression of some SSP enzyme transcripts is greater in B cells deprived of serine and glycine

There was no difference in B cell proliferation or viability when depriving B cells of serine/glycine. I therefore focused on determining if the SSP was upregulated in response to serine/glycine deprivation. I carried out qPCR for SSP enzymes at 24 and 48 hours, to determine how transcript levels of SSP enzymes change over a time course. Splenic B cells isolated from WT mice were stimulated with ODN-1826 and anti-CD40 agonistic antibody. I calculated gene expression in serine/glycine deprived conditions relative to serine/glycine supplemented conditions. Greater Phgdh and Psat1 transcript expression was identified in B cells deprived of serine and glycine, compared to serine and glycine supplemented conditions (Figure 8). Shmt1, Shmt2, and Aicda did not appear to change between the serine/glycine replete or deplete conditions (Figure 8). Statistical analysis or fold change interpretation could not be carried out on this data as day 0 samples were not available to use as baseline gene expression.

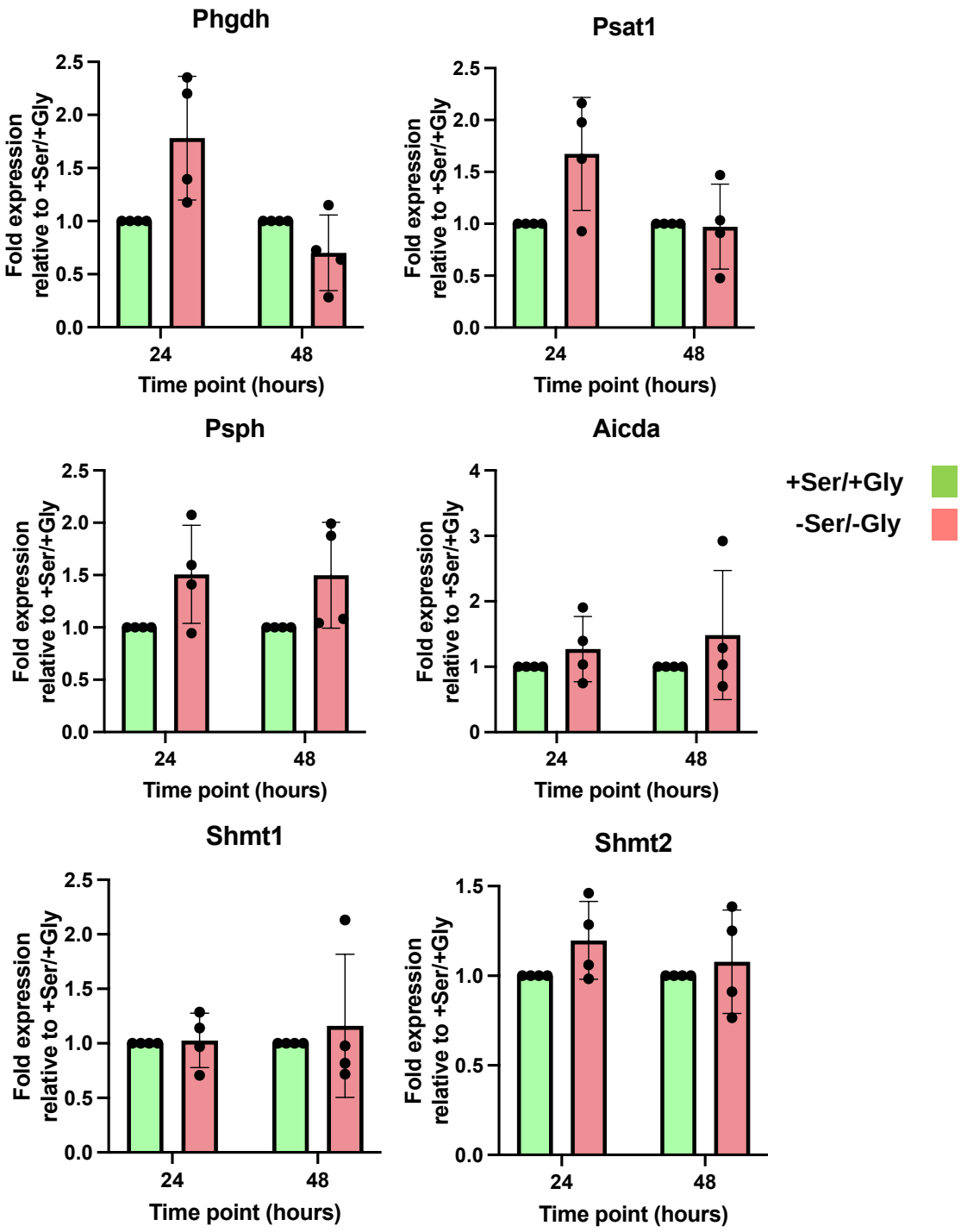

Figure 8 - SSP gene transcription increases more in serine/glycine deprived conditions at 24 hours post-stimulation.

mRNA expression of B cells cultured in different serine/glycine conditions at distinct time points (hours). Cells were stimulated with ODN1826 and anti-CD40. In all graphs, n=4 with 2 biological replicates, carried out over 2 independent experiments. All -Ser/-Gly data is normalised to +Ser/+Gly, to determine fold difference.

1.3 – Serine and glycine deprived B cells show greater expression of SSP proteins

qPCR analysis indicates there may be an increase in Phgdh and Psat1 gene expression in B cells deprived of serine/glycine at 24 hours. To determine if these genes were being translated, I carried out a western blot for these SSP enzymes. Isolated splenic B cells from WT mice were stimulated with CpG and anti-CD40 agonistic antibody. Western blotting for PHGDH and PSAT1 was carried out on protein isolated at 72 hours, with α-Tubulin used as a loading control (Figure 9A). In cells deprived of serine/glycine, I saw a slight but non-significant increase in PHGDH (Figure 9B), however a significant increase in PSAT1 (Figure 9C) was detected.

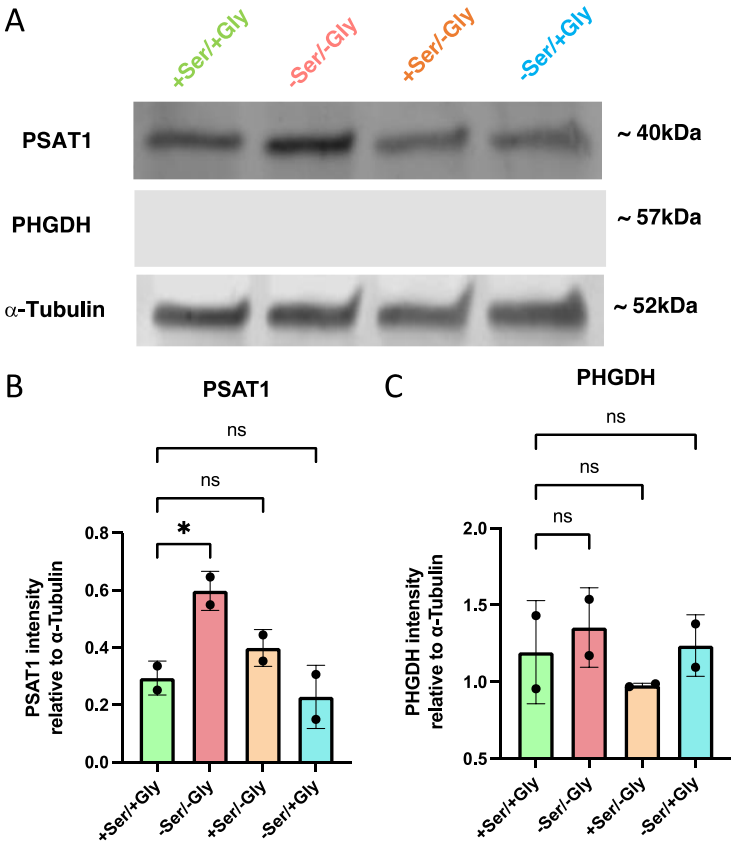

Figure 9 - Serine and glycine deprivation increases PSAT1 levels 72 hours post-stimulation.

A) Representative western blot showing bands for PSAT1, PHGDH and α-Tubulin from B cells cultured in different serine/glycine conditions and stimulated with ODN1826 and anti-CD40. B) PSAT1 quantification relative to the loading control, α-tubulin C) PHGDH quantification relative to the loading control, α-Tubulin. n=2, carried out over 2 independent experiments. Statistical analysis was carried out using one-way ANOVA. For statistical analysis, non-significance (ns) = $P \geq 0.05$ and * = $P \leq 0.05$.

I next wanted to determine how SSP enzymes are expressed over a time course. To do this, I carried out western blotting on protein from 4 distinct timepoints: 0, 24, 48 and 72 hours, stimulating isolated splenic B cells with ODN1826 and anti-CD40 agonistic antibody (Figure 10A). I identified PHGDH and PSAT1 to be upregulated in activated B cells regardless of whether they were deprived of or supplemented with serine/glycine, where greater upregulation was observed in the serine/glycine deprived condition (Figure 10B and C). However, even though an increase can be seen in both conditions, there is no significance when comparing conditions, most likely due to variation between experiments. The increase between time points within conditions could be significant. This indicates that activation of B cells causes upregulation of the SSP, which may be more greater in the absence of exogenous serine and glycine.

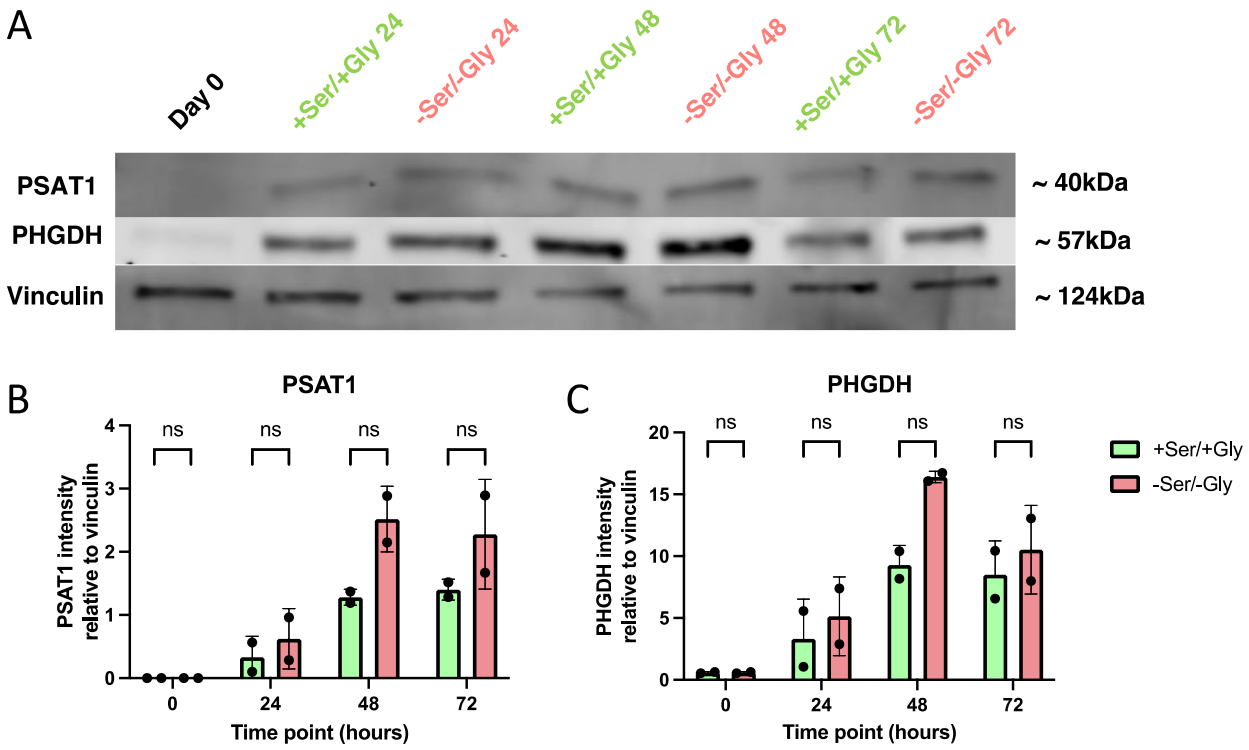

Figure 10 - Serine and glycine deprivation results in greater SSP levels over a 72-hour time course.

A) Representative western blot images showing bands for PSAT1, PHGDH and Vinculin in B cells cultured in serine/glycine deplete or replete conditions, stimulated with ODN1826 and anti-CD40 agonistic antibody, over 3 distinct timepoints. B) PSAT1 quantification relative to the loading control, Vinculin. C) PHGDH quantification relative to the loading control, Vinculin. n=2, with a biological replicate from 2 independent experiments. Statistical analysis was carried out using two-way ANOVA. For statistical analysis, non-significance (ns) = $P \geq 0.05$.

1.4 – IgM secretion is not affected in B cells deprived of serine and glycine

Since serine/glycine deprivation does not decrease the proliferative capacity of B cells, I wanted to investigate whether B cell function was affected. I performed an ELISA for IgM on cell culture supernatant from B cells stimulated with anti-CD40 agonistic antibody and IL-4 for 72 hours. Cells were counted and IgM secretion per cell was calculated to normalise for total cell number. Whether serine or glycine were present or not in the media, there was no statistical difference in IgM secretion (Figure 11).

No statistical significance is very likely due to inter-experimental variation. Further repeats would be required to ensure robustness of the data.

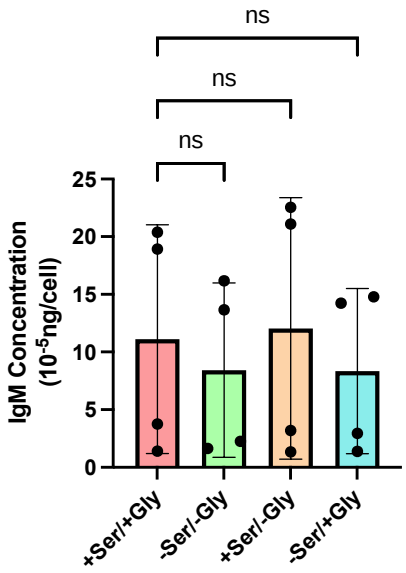

Figure 11 - IgM secretion does not change during serine and/or glycine deprivation.
IgM secretion per cell from B cell culture media in different serine/glycine conditions. B cells were stimulated with IL-4 and anti-CD40 agonistic antibody over 72 hours. n=4 with 4 biological replicates over 3 independent experiments. Statistical analysis was carried out using one-way ANOVA. For statistical analysis, non-significance (ns) = $P \geq 0.05$, * = $P \leq 0.05$ and ** = $P \leq 0.01$.

1.5 – Inhibition of PHGDH increases dependency on exogenous serine and glycine

PHGDH is the rate-limiting enzyme of the SSP (120). I inhibited PHGDH using the non-competitive pharmacological inhibitor, NCT-503, to determine how B cell proliferation and viability was affected by inhibition of the SSP (149). I stimulated B cells with anti-CD40 agonistic antibody and IL-4 in the presence of a range of NCT-503 concentrations, from 10μM to 40μM. I analysed cell division of live CD19+ B cells. I saw an NCT-503 dose-dependent reduction in proliferation in cells deprived of serine/glycine (Figure 12A). Viability decreased at higher concentrations of NCT-503, although B cells were more viable during serine/glycine supplementation than serine/glycine deprivation. (Figure 12B). This data indicates increased dependency on exogenous serine and glycine when PHGDH is pharmacologically inhibited.

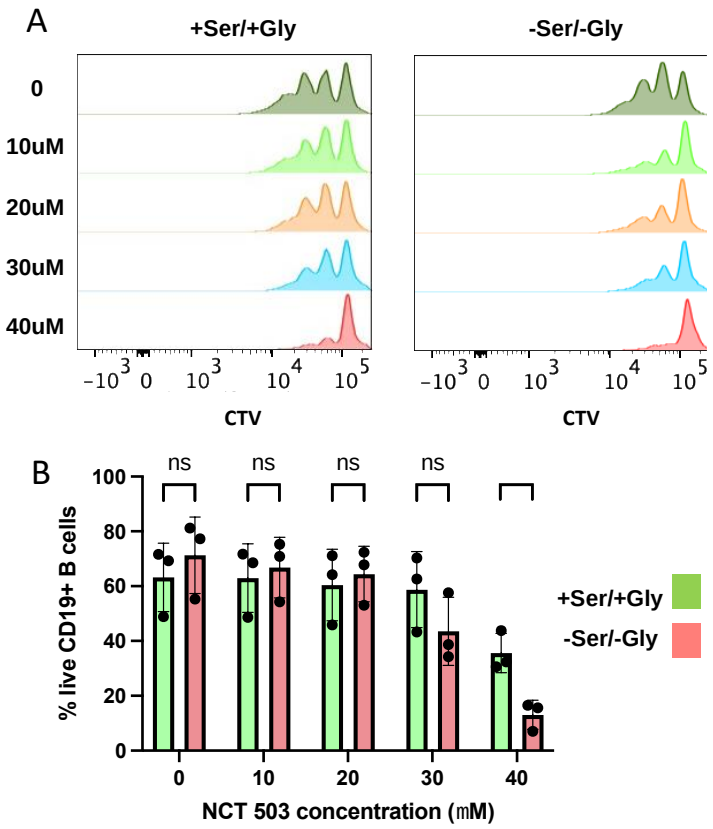

Figure 12 - Pharmacological inhibition of PHGDH increases dependency on exogenous serine and glycine.

A) CTV histogram plot of B cells cultured in different serine/glycine conditions, in the presence of variable concentrations of NCT-503. B) Cell viability of B cells cultured in different serine/glycine conditions, in the presence of variable concentrations of NCT-503. n=6, with 3 biological repeats over 2 independent experiments. Statistical analysis was carried out using two-way ANOVA. For statistical analysis, non-significance (ns) = $P \geq 0.05$, * = $P \leq 0.05$, ** = $P \leq 0.01$ and *** = $P \leq 0.001$.

1.6 – B cell division, but not viability, is reduced during ser/gly deprivation under low-glucose conditions

The glycolytic intermediate, 3-PG, feeds into the SSP by being converted to 3-PHP by PHGDH. To seek further evidence of dependence on the SSP in serine/glycine deprived B cells, I cultured B cells in a range of glucose concentrations with or without serine/glycine, with anti-CD40 agonistic antibody and IL4 stimulation. I saw no significant changes in viability between the two conditions at different glucose concentrations (Figure 13A). However, cell division was affected by serine/glycine deprivation at low glucose concentrations (Figure 13B). Overall, cells cultured in serine/glycine supplemented conditions displayed a significantly higher division index, compared to serine/glycine deprived conditions.

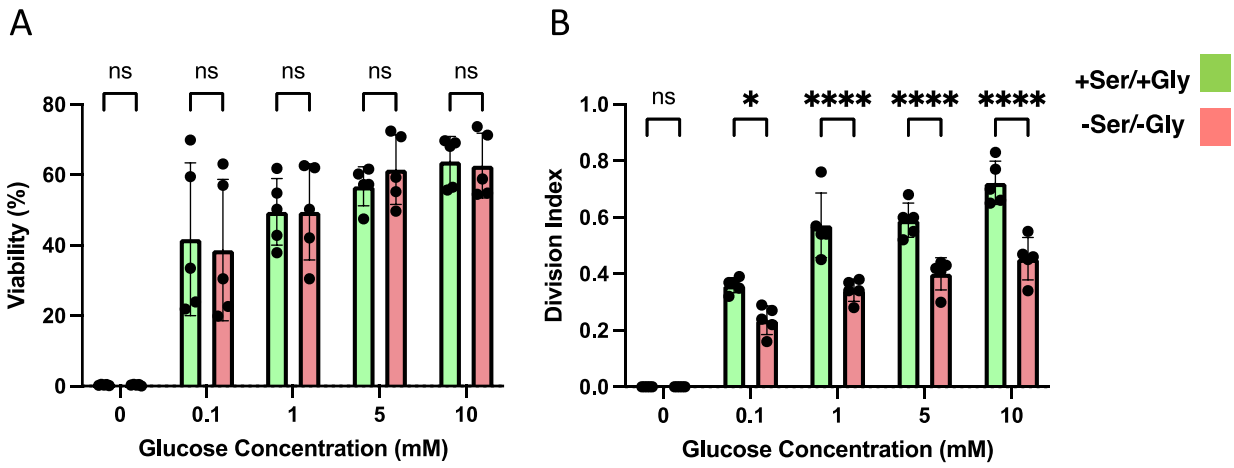

Figure 13 - Glucose affects division of serine and glycine deprived B cells, but viability is maintained.
A) Viability of B cells cultured in different serine/glycine conditions in a range of glucose concentrations, stimulated with IL4 and anti-CD40 agonistic antibody. B) Division index of B cells cultured in different serine/glycine conditions in a range of glucose concentrations. n=5, with 5 biological replicates from 2 independent experiments. For both graphs, a two-way ANOVA was conducted. For statistical analysis, non-significance (ns) = $P \geq 0.05$, * = $P \leq 0.05$ and **** = $P \leq 0.0001$.

2 – The effects on serine and glycine deprivation on B cell differentiation and immunoglobulin class switching

2.1 – A relative decrease in immunoglobulin class switching is observed in B cells deprived of serine and glycine

I stimulated isolated splenic B cells from WT mice with LPS, anti-CD40 agonistic antibody, IL-4 and IL-21, with and without serine and glycine over 4- and 6-days. LPS triggers B cell immunoglobulin class switching towards IgG1 and IL-21 promotes differentiation towards plasmablasts (24,150). The representative gating strategy for this experiment shows my populations of interest gated from live B cells: CD138+ plasmablasts, CD138+IgG1+ plasmablasts, IgD+ B cells, IgM+ B cells and IgG1+ B cells (Figure 14A). Overall no statistical significance was identified between conditions in any of the populations, which may have been caused by inter-experimental variation. However, we do see a decrease in viability, as well as live IgM+ and live IgD+ B cells from day 4 to day 6, in both serine/glycine conditions (Figure 14B, C and D). The percentage of IgG1+ B cells increases in both conditions from day 4 to day 6, however during serine/glycine deprivation, it tends to be less than cells supplemented with serine/glycine. (Figure 14E) The difference in plasmablasts is very small, with an increase being identified in serine/glycine deprived conditions (Figure 14F). IgG1+ plasmablasts tend to not be different on day 4 or 6 between both conditions (Figure 14G). Further repeats and elimination of outlier data would be required to make final conclusions on this experiment. Furthermore, absolute cell counts would be required to determine the actual effect of serine/glycine deprivation on B cell populations.

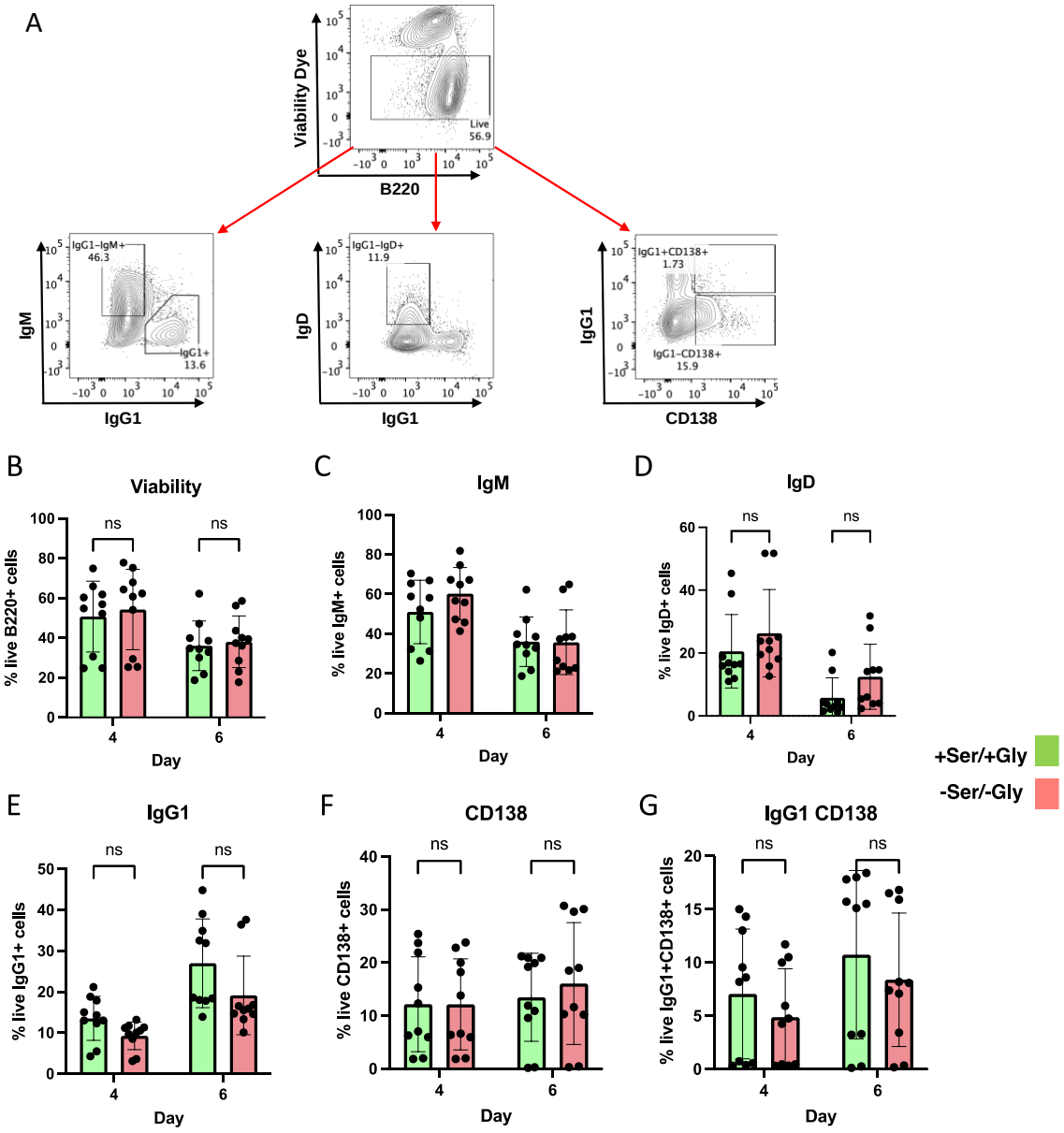

Figure 14 - Less IgG1+ B cells during serine/glycine deprivation, compared to serine/glycine supplementation.

A) Representative gating strategy of B cell populations of interest. B) B cell viability from different serine/glycine conditions on day 4 and 6. C) IgM+ B cells from different serine/glycine conditions on day 4 and 6. D) IgD+ B cells from different serine/glycine conditions on day 4 and 6. E) IgG1+ B cells from different serine/glycine conditions on day 4 and 6. F) CD138+ plasmablasts from different serine/glycine conditions on day 4 and 6. G) CD138+IgG1+ plasmablasts from different serine/glycine conditions on day 4 and 6. n=10, with 10 biological replicates from 4 independent experiment. For all graphs, a two-way ANOVA was conducted. For statistical analysis, non-significance (ns) = $P \geq 0.05$.

3 – Conditional PHGDH deletion in B cells causes an increase in immunoglobulin class switching towards the IgG1 isotype

3.1 – B cell conditional Phgdh deletion increased IgG1 expression post-SRBC immunisation

To determine if Phgdh deletion was effective, I carried out western blotting for PHGDH on B cells from WT and Phgdh KO mice, stimulated with ODN1826 and anti-CD40 agonistic antibody for 24 hours. There was no band for PHGDH, confirming disruption of the Phgdh gene in Mb1-cre Phgdh-flox mice (Figure 15A). Conditional Phgdh-KO mice and WT litter mate controls were immunised with sheep red blood cells (SRBC) and splenic B cells were analysed at day 9. Flow cytometry was carried out to distinguish MZ and Fo B cells, using the surface markers CD21 and CD23, on live CD19+ B cells (Figure 15B). Flow cytometry was also carried out to identify plasma cells (CD138+TACI+) and GC B cells (GL7+CD38-) from pre-gated live B cells (Figure 15C). Within GC B cells, I also gated DZ and LZ (CD86 low and CXCR4 high, and CD86 high and CXCR4 low respectively) and IgG1+ GC B cells (CD19+IgG1+) (Figure 15C). Percentage cell populations were quantified in the relevant plots (Figure 15D-J). The only populations displaying a significant difference are IgG1+ GC B cells (Figure 15H) and follicular (Fo) B cells (Figure 15I). There was a small but statistically significant increase in Fo B cell proportions in Phgdh KO mice. IgG1+ B cells were significantly increased in Phgdh KO mice.

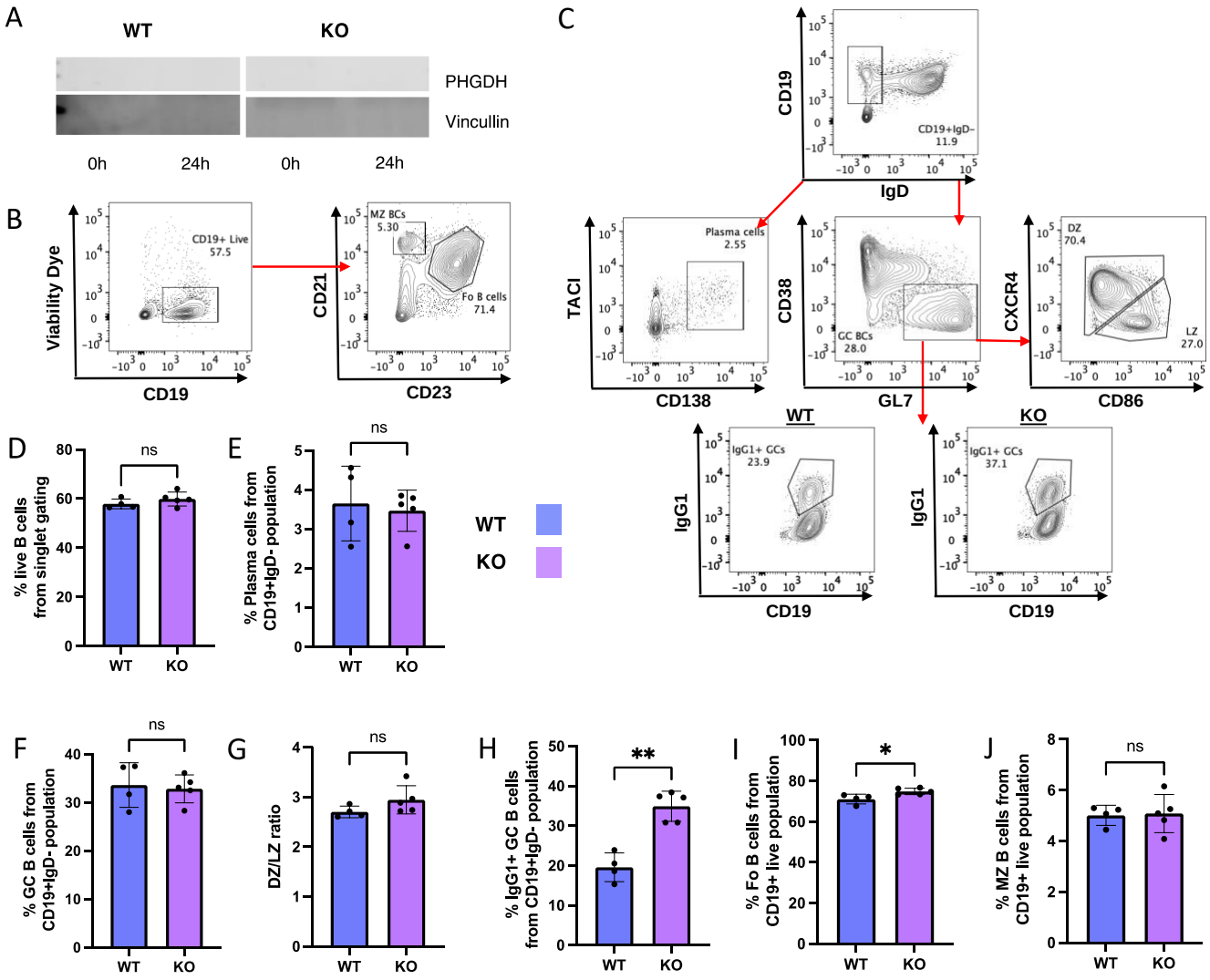

Figure 15 - Conditional Phgdh KO in B cells results in a relative increase in IgG1+ GC B cells in vivo.

A) Confirmation of Phgdh KO by western blotting. B**)** Gating strategy of CD23+CD21int Fo B cells and CD23-CD21+ MZ B cells. C) Gating strategy of GL7+CD38- GC B cells, IgG1+ GC B cells, CD86-CXCR4+ DZ and CD86+CXCR4- LZ, CD138+TACI+ Plasma cells, pre-gated on live B cells D) Percentage viability of WT and KO mice B cells. E) Percentage plasma cells from WT and KO mice. F) Percentage GC B cells from WT and KO mice. G) DZ/LZ ratio from WT and KO mice. H) Percentage IgG1+ GC B cells from WT and KO mice. I) Percentage Fo B cells from WT and KO mice. J) Percentage MZ B cells from WT and KO mice. 4 WT and 5 KO mice over 1 experiment. Statistical analysis was carried out using an unpaired T test. For statistical analysis, non-significance (ns) = $P \geq 0.05$, * = $P \leq 0.05$ and ** = $P \leq 0.01$.

3.2 – Phgdh conditional-KO mice show increased IgG1+ B cells in vitro

Splenic B cells from Phgdh conditional-KO mice and WT litter mate controls were cultured with LPS, anti-CD40 agonistic antibody, IL-4 and IL-21 for 4- and 6-days. Phgdh-KO B cells died without serine/glycine supplementation, therefore the data for this experiment consists of cells cultured with serine/glycine. The representative gating strategy for this experiment shows my populations of interest: CD138+ plasmablasts, CD138+IgG1+ plasmablasts, IgD+ B cells, IgM+ B cells and IgG1+ B cells (Figure 16A). Representative CTV histogram plots for WT and KO mice on both days indicates no effect on proliferation (Figure 16B). There was no difference between KO and WT mice in cell viability, IgD+ B cells, CD138+ plasmablasts or CD138+IgG1+ plasmablasts (Figure 16C, F, G, and H). Both WT and KO mice displayed decreased IgM+ B cells, with the decrease being more significant in KO mice (Figure 16D). Surface IgG1+ on B cells on day 6 increased in both KO and WT mice (Figure 16E). The increase in surface IgG1 between day 4 and 6 was greater in KO mice (Figure 16E). This relative decrease in IgM and relative increase in IgG1 may indicate increased immunoglobulin class switching (Figure 16H), which is a finding similar to that of immunised Phgdh-KO mice, which display relatively increased IgG1+ GC B cells. A way to measure this would be to determine how much IgG1 and IgM is being expressed on the cell surface initially prior to cell culture. Another reasoning behind the increase in IgG1+ B cells could be increased survival, where IgM expressing cells may be dying. To determine this, I could look at absolute cell counts and working out relevant proportions of each population.

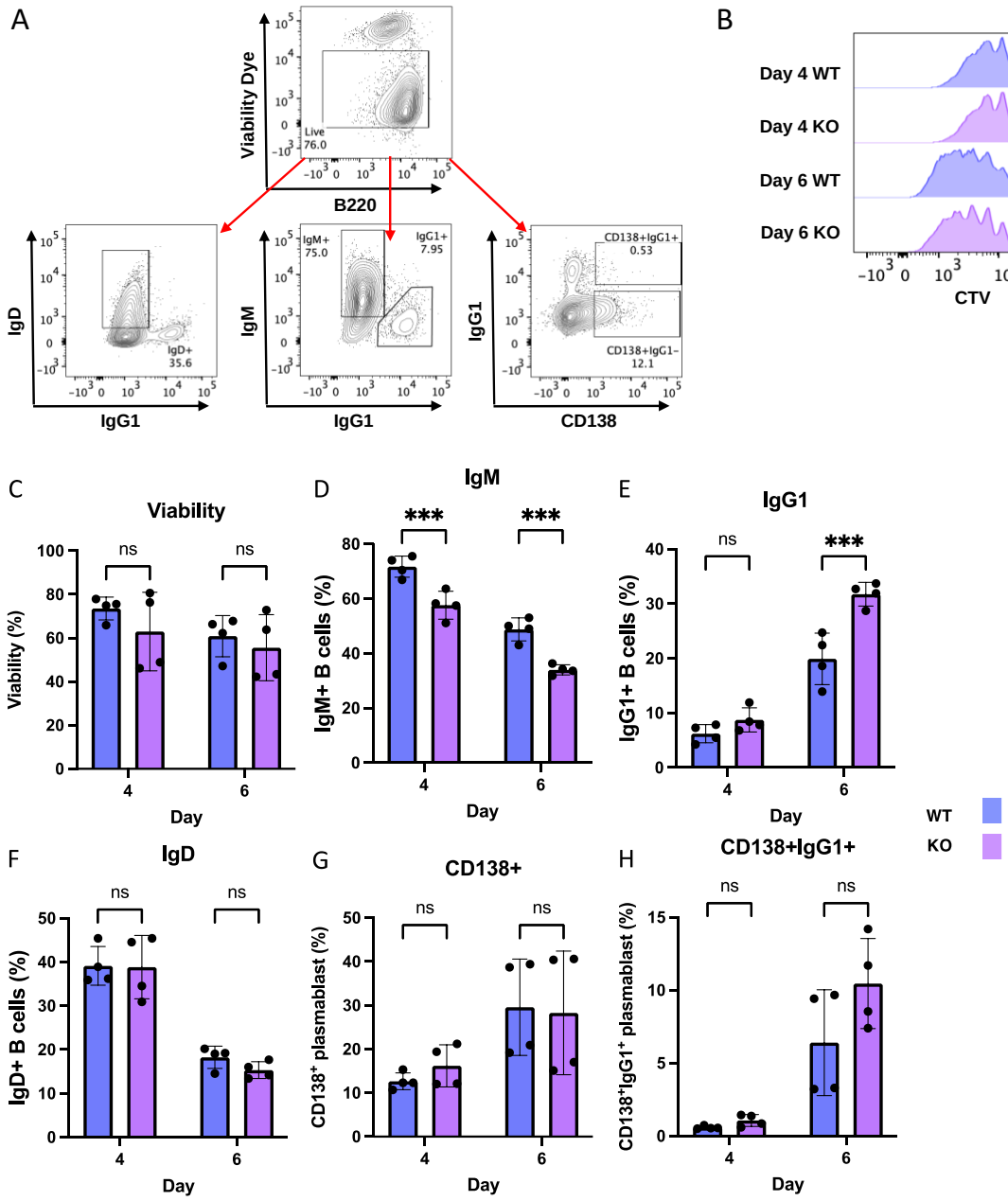

Figure 16 - Conditional Phgdh KO in B cells causes a relative increase in IgG1+ B cells in vitro.

A) Representative gating strategy of B cell populations of interest. B) CTV proliferation plots of live WT and KO B cells on day 4 and day 6. C) B cell viability from WT and KO mice on day 4 and 6. D) IgM+ B cells from WT and KO mice on day 4 and 6. E) IgG1+ B cells from WT and KO mice on day 4 and 6. F) IgD+ B cells from WT and KO mice on day 4 and 6. G) CD138+ B cells from WT and KO mice on day 4 and 6. H) CD138+IgG1+ B cells from WT and KO mice on day 4 and 6. 4 WT mice and 4 KO mice were used from 2 independent experiment. For all graphs, a two-way ANOVA was conducted. For statistical analysis, non-significance (ns) = $P \geq 0.05$, * = $P \leq 0.05$, ** = $P \leq 0.005$ and *** = $P \leq 0.001$.

3.3 – IgM secretion is not affected between Phgdh conditional-KO mice or WT mice

To see if IgM secretion of B cells was affected by PHGDH, I conducted an IgM ELISA on the culture medium from experiment 3.2, for both WT and KO mice. Media was taken from different wells for the two timepoints. IgM secretion decreases from day 4 to day 6 in both WT and KO mice however, was no significant difference in IgM secretion between WT or KO mice (Figure 17).

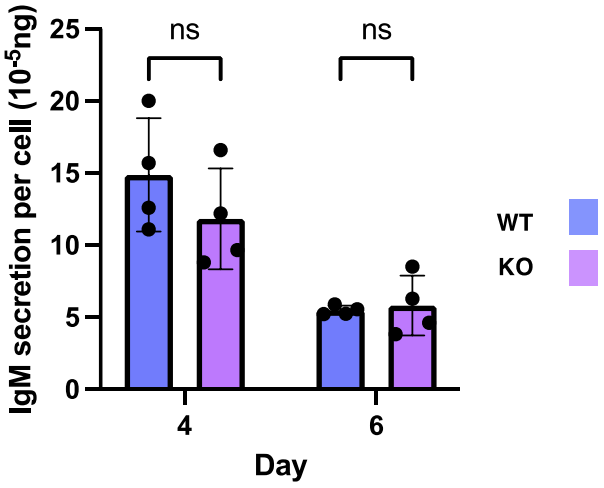

Figure 17 - No difference in IgM secretion between WT and Phgdh-KO B cells.
IgM secretion per cell from culture media of B cells cultured for 4- or 6-days from WT or KO mice. B cells were stimulated with anti-CD40, IL4, IL21 and LPS. 4 WT mice and 4 KO mice were used from 2 independent experiment. Statistical analysis was carried out using two-way ANOVA. For statistical analysis, non-significance (ns) = $P \geq 0.05$.

3.4 – H3K4Me3 increases in Phgdh-KO B cells

The SSP feeds into the 1C metabolism cycle, which branches off into the methionine cycle. SAM is an important methyl donor (120,128). To determine if there was less methylation as a result of inhibiting the SSP, I carried out a time point western blot of histone H3 and the histone methylation marker, H3K4me3, in WT and KO mouse B cells (Figure 18A). Total histone H3 protein increased in both WT and KO B cells over the initial 48 hours, although KO B cells displayed higher total histone H3 at day 0 (Figure 18B). H3K4Me3 is a marker that upregulates the transcription of Aicda (151). I carried out western blotting of H3K4Me3, and revealed a gradual increase in WT mice over 72 hours, whereas KO mice increased their expression initially at 48 hours and increased it even further at 72 hours (Figure 18C). When quantifying the ratio of H3K4me34 to total H3, I still found increased methylation in KO mice (Figure 18D). This experiment is provisional and requires further replication which I did not have time to do.

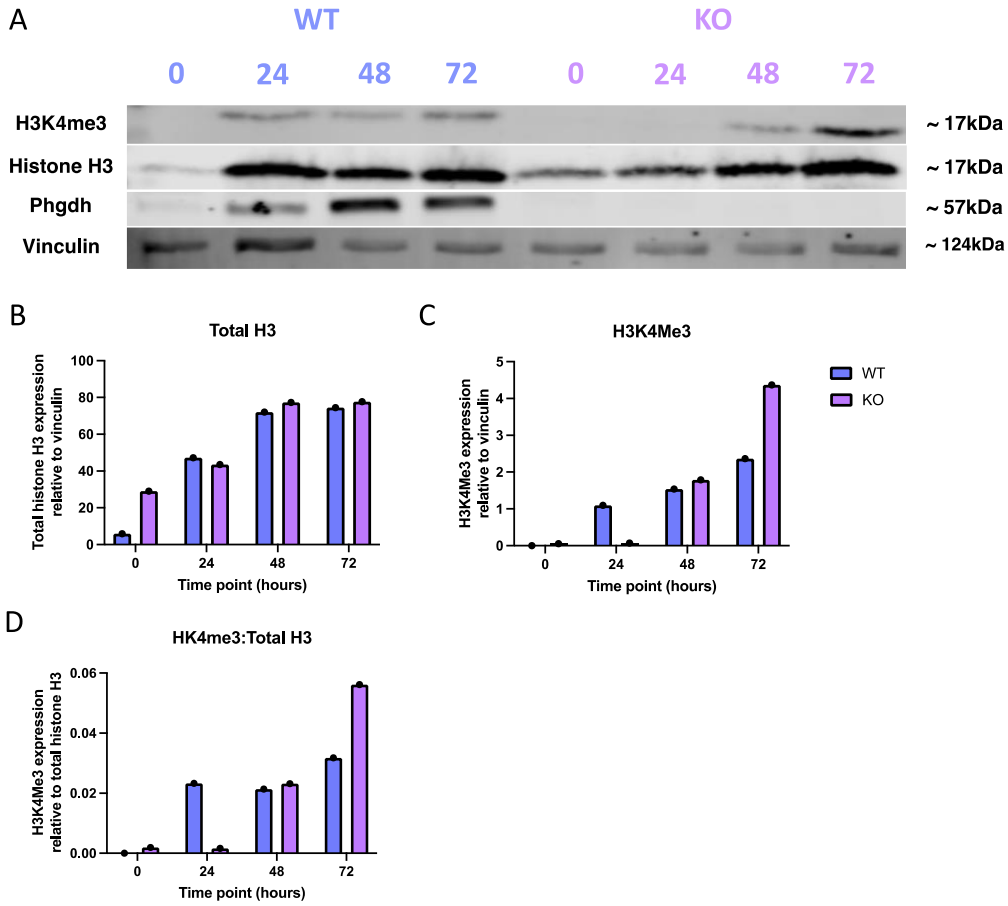

Figure 18 - H3K4me3 increases in Phgdh-KO B cells.
A) Representative western blot showing bands for H3K4Me3, Histone H3, Phgdh and Vinculin in WT and KO mouse B cells at distinct time points. B cells were stimulated with CpG ODN1826 and anti-CD40. B) H3K4Me3 quantification relative to the loading control, vinculin. C) Histone H3 quantification relative to the loading control, Vinculin. n=1 for WT and n=1 for KO carried out over 1 experiment.

3.5 – Protein synthesis does not differ between WT and Phgdh-KO B cells

O-propargyl-puromycin (OPP) is a puromycin alkyne analogue which can be integrated into newly synthesized proteins. I therefore took advantage of this system to determine if protein synthesis was affected in Phgdh KO B cells. OPP expression was analysed by gating on live B220+ B cells (Figure 19A). gMFI was calculated for both WT and KO B cells (Figure 19B). From this data, it is evident that OPP is not changed between KO and WT B cells.

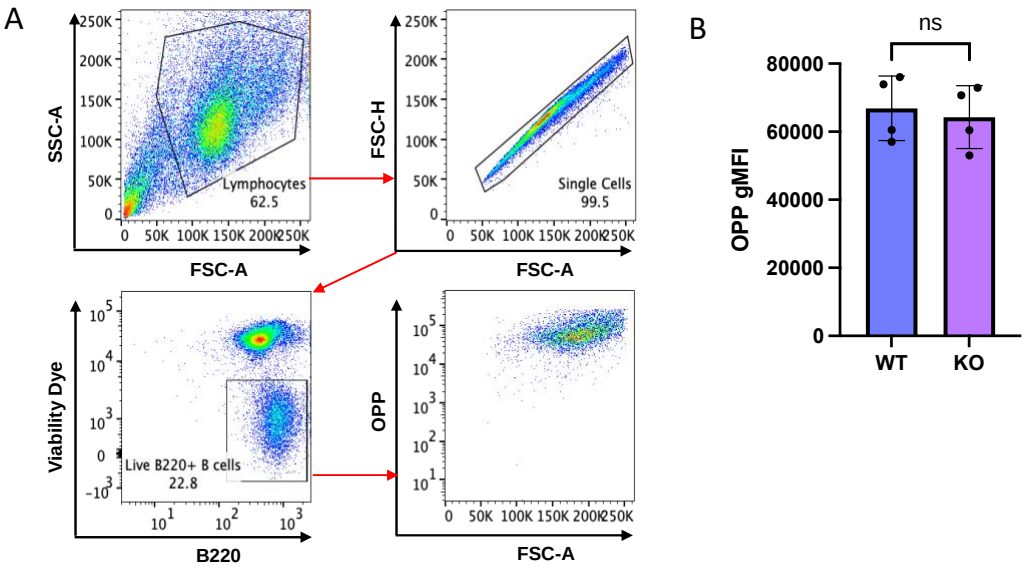

Figure 19 - Protein synthesis does not change in Phgdh KO B cells.
A) Gating strategy of OPP fluorescence from live B cells stimulated with anti-CD40 agonistic antibody and IL4. B) OPP gMFI in WT and KO mice. n=4, with 4 biological replicates, over 2 independent experiments. Statistical analysis was carried out using an unpaired T-test. For statistical analysis, non-significance (ns) = $P \geq 0.05$

Discussion and conclusions

In this thesis, I have shown that B cells upregulate the SSP during activation which is required for their proliferation and differentiation. No difference was identified in viability or proliferation of B cells cultured over 3 days with serine/glycine, without serine/glycine, with serine only and with glycine only. Consistent with this finding, B cells also upregulated PHGDH and PSAT1 during activation. Upregulation of these enzymes was greater in the serine/glycine deplete condition than the serine/glycine supplemented condition at protein levels over a 3-day time course. Fold difference of Phgdh and Psat1 was higher in serine/glycine deprived conditions at the transcript level, although statistical analysis could not be carried out, as a result of lack of day 0 conditions to compare the values to. IgM secretion was reduced slightly, but not significantly, in B cells cultured in serine deprived conditions. An assumption behind this may be the ISR is activated when serine deprivation is detected, and uncharged tRNAs activate GCN2 (123,152). GCN2 reduces protein synthesis through phosphorylation of eIF2α, which then cannot bind to ribosomal structures required for translation (123,152). B cells may reduce immunoglobulin synthesis through this manner**.** It would be interesting to see whether B cells stimulated with anti-CD40 and IL-4 over 3 days also reduces surface IgM or intracellular IgM levels. Since plasmablasts are involved in secretion of immunoglobulin, their differentiation may be affected by serine/glycine deprivation and may be worth investigating through flow cytometry in a 3-day cell culture. Inhibiting PHGDH using NCT-503 led to reduced viability in both conditions, with serine/glycine deprived B cells being more greatly affected. Whilst the effects of the inhibitor may be off target, resulting in toxicity and hence reducing B cell viability, this also demonstrates B cells have some dependency on exogenous serine/glycine when the SSP is blocked. It would be worth investigating

the effects on viability and proliferation at lower dosage of NCT-503 also.

Decreasing glucose concentrations in B cell culture media had an impact on cell division. When decreasing glucose concentrations in both serine/glycine deplete and replete conditions, I saw a reduction in cell division. This would be explained by a requirement for glycolysis during B cell activation (83,85,87). B cells deprived of serine/glycine had significantly lower cell division in all glucose concentrations, compared to the serine/glycine supplemented conditions. Interestingly, B cell viability was not affected by the presence or absence of serine/glycine. Assuming that the SSP is upregulated in B cells deprived of serine/glycine, I would expect flux through the 1C metabolic pathway. Most of the *de novo* serine may be shunted towards survival mechanisms, such as GSH production, since B cell activation is known to rapidly increase ROS (100,101). With reducing glucose concentrations, B cells may prioritise glycolytic flux over other pathways to maintain essential metabolic pathways, thus reducing proliferation. OXPHOS has been identified to be upregulated in activated B cells and glucose restriction does not affect activated B cell function, which may explain the maintained viability between serine/glycine supplemented and deprived conditions (87). To test the contribution of 3-PG towards SSP and glycolysis, B cells could be cultured with ^{13}C-labelled glucose, which can then be measured by mass spectrometry. Additionally, B cell glycolysis and OXPHOS can be measured through the metabolic Seahorse assay, helping to determine the effects between the different serine/glycine conditions. Counting cells at the end of the cell culture, before analysing in this experimental set up, will help me to identify whether cell division was affected.

Cells cultured between 4- and 6-days display an increased percentage of IgG1+ B

cells, although cells deprived of serine and glycine had a slightly smaller percentage of IgG1+ B cells. Between day 4 and day 6, I saw a reduction in viability, IgD and IgM. This could indicate multiple things, one of them being increased cell death of rapidly dividing cells or cell death of non-class-switching cells. Another assumption may be to do with increased class switching of cells or increased proportion of class switched cells which are not dying. Since I did not have cell counts for each condition, I cannot assume that the absolute cell count is increased or decreased and therefore the percentages of these populations are relative. An explanation behind the relative increase in the CD138+ plasmablast population may be to do with glycolytic flux. As SSP enzymes increase in response to serine/glycine deprivation, flux through the SSP may therefore increase and less glycolytic intermediates may form downstream of 3-PG. Plasmablasts may therefore be switching towards OXPHOS as a pathway to generate ATP. As activated B cells differentiate towards becoming plasmablasts, it has been shown that there is a switch from glycolysis towards OXPHOS (109). Measuring OXPHOS through the flow cytometry metabolic assay, SCENITH, would allow me to determine the effects of inhibiting glycolysis and OXPHOS through calculating OPP incorporation. Alternatively using the Seahorse assay would provide further information about glycolytic or OXPHOS metabolism of B cells during serine/glycine deprivation or supplementation. Testing to see if other IgG isotypes, IgA, or IgE differ would allow for further clarification as to whether it affects switching to other subclasses or if it is specific to IgG1.

Immunising Mb1-Cre Phgdh-Flox mice allowed me to analyse the effects of Phgdh conditional-KO on B cells in vivo. After a 9-day immunisation with a single dose of SRBC, the only significant difference identified was an increase in IgG1+ GC B cells

in KO mice and a very small difference in follicular B cells. This was a similar finding to that I identified in vitro, where I saw a relative increase in IgG1+ B cells and relative reduction in IgM+ and IgD+ B cells. It is important to note that PHGDH-KO B cells stimulated in vitro did not survive in serine/glycine deplete conditions and therefore required supplementation with serine/glycine for in vitro experiments. B cells increase ROS during activation and the SSP produces GSH (100,101). If flux through the SSP cannot occur, I assume excessive oxidative stress would be present, leading to B cell death. However, this is the opposite of what I saw when I deplete serine/glycine from WT B cells in the same experimental conditions in chapter 2, where I identified IgG1+ B cells to be reduced, relative to IgM+ and IgD+ B cells. Since WT B cells can survive and proliferate despite serine/glycine depletion, by upregulating the SSP, I assume the increase in IgG1+ B cells is a PHGDH-KO specific phenotype. ROS have been identified in increasing B cell CSR through downregulation of heme (103). Assuming there is reduced 1C flux and therefore less GSH, increased ROS may be involved in the increased proportion of IgG1+ GC B cells in vivo and increased proportion of IgG1+ B cells in vitro. B cell viability decreased in the absence of serine/glycine at high NCT-503 concentrations, as demonstrated in an earlier experiment. The dependency on exogenous serine/glycine in PHGDH-KO B cells and during pharmacological PHGDH inhibition highlights the importance of serine/glycine for survival and proliferation.

IgM secretion reduced from day-4 to day-6 during in vitro stimulation of both WT and Phgdh KO, although no difference was identified between WT or KO mice. When attempting an ELISA to determine IgG1 secretion in Phgdh KO mice, I was unable to detect IgG . This was attempted numerous times with different troubleshooting, which did not seem to fix the detection issue. IL-4 is known to be involved in B cell class

switching towards IgG1 and IgE (153). The concentrations of IL-4 may have been too low. LPS also leads to IgG1 class switching, and its concentration may also not have been optimal. IL-4 and LPS concentrations could be increased to determine if this was affecting IgG1 secretion. When analysing OPP uptake between WT and KO mice stimulated in vitro, I saw no difference in gMFI, indicating no defect in protein synthesis. This may indicate no ISR in Phgdh KO mouse B cells, because they were cultured in serine/glycine replete media. If the ISR was activated, I would expect attenuation of global protein synthesis as a consequence (154). Since there is no difference in OPP uptake in KO mice, OPP uptake requires investigating in B cells deprived of serine/glycine, to determine if the assumed decrease in relative immunoglobulin expression is triggered by the ISR pathway. Western blotting analysis for histone methylation in Phgdh KO mice indicates higher levels of total histone H3 protein over a time course post-activation. This was also seen with H3K4me3, a methylation mark which has been associated with increased Aicda transcription (42). If methylation marks associated with increased Aicda expression were increasing, I would expect repression marks associated with Aicda , such as H3K9Me3 or H3K27me3, to consequently decrease (42). In further experiments, measurement of repressive methylation marks through western blotting would help me to determine this. Aicda gene expression and AID protein levels would need to be measured to determine if this was the cause. The interesting finding here is the increased methylation in the absence of 3-PG flux through the SSP. With less flux through the 1C cycle, it is not expected that levels of SAM, a major methyl donor, would be higher. To determine if this is a true finding, further experimental replication is required.

A paper published during the conclusion of my project, by D'Avolo et al., looked at the

SSP in GCs (146). Similar to my findings, they found unstimulated naïve B cells to have minimal expression of SSP enzymes compared to in vitro activated B cells, which had increased PHGDH and PSAT1 over a time-course, however they also stimulated their cells through the BCR with anti-IgM/G. Wang et al., also showed upregulation of SSP enzymes in EBV-infected B cells, which subsequently supports the synthesis of biosynthetic building blocks for proliferation (99). It is clear that the SSP increases upon stimulation, even more so in serine/glycine deplete conditions. One of the key findings by D'Avolo et al. that opposes my work is that genetic ablation of Phgdh results in impaired Ig class switching and GC formation post SRBC immunisation. There are a number of differences in approaches between my work and their paper. Firstly, their cre was under the promoter of CD19, whereas mine was under Cd79a. Both genes are expressed early in B cell development. As Mb-1-cre is a more efficient cre, it is unlikely this was the cause of the difference in results obtained. Another difference is the way in which their immunisation was delivered. They administered SRBC intravenously, whereas we injected mice intra-peritoneally. Intravenous injections directly enter the systemic circulation, leading to high levels of SRBC accumulation in the spleen. The increased number and size of GCs may lead to differences in metabolic demands and hence higher requirement for serine synthesis. Differences in microbiomes between mice housed in differing environments may also be relevant.

A broader approach to take in further experiments to use ^{13}C-glucose and ^{13}C-serine tracing in vivo to determine how incorporation takes place in WT and Phgdh KO mice. Mice could be injected into the tail vein with ^{13}C-glucose or ^{13}C-serine, or alternatively, could be provided in a liquid form to the mice to ingest. This approach could also be

used in vitro to determine how B cells utilise exogenous glucose and serine during serine/glycine supplementation or deprivation. mTORC1 is the central mechanism for cells to detect the availability of amino acids and make the intracellular changes required. Another experiment that would provide us with further information about the metabolic dynamics in B cell differentiation is immunising mice with a booster dose of SRBC. This would provide me with further information as to whether memory B cells are affected by PHGDH inhibition. A population of mTORC1 low GC B cells have been found to favour memory-B cell formation (113). Upon a further immunisation, if mTORC1 is downregulated, an increase in memory B cells may be observed.

Pharmacologic inhibition or genetic ablation of Phgdh, with removal of serine/glycine from cell media, has been demonstrated to be most effective in reducing B cell viability and proliferation in mouse models. This may have translational relevance, where patients displaying autoimmune diseases or cancer with upregulated SSP could be treated using a combination of drugs inhibiting the SSP with a serine/glycine-free diet. This has been demonstrated to be effective in cancer treatment, where dietary restriction of serine and glycine improved cancer drug treatment (155,156). D'Avolo et al. showed the SSP to be upregulated by MYC in a B cell lymphoma. Blocking PHGDH resulted in apoptosis of Burkitt lymphoma B cell lymphoma, as a result of less serine synthesis and decreased proliferation (146). Being able to target B cells through the SSP, a pathway that is highly upregulated and contributes to essential cellular pathways and biosynthetic material make up, may help control disease progression.

Bibliography

1. Kim CH, Rott LS, Clark-Lewis I, Campbell DJ, Wu L, Butcher EC. Subspecialization of Cxcr5+ T Cells. J Exp Med. 2001 Jun 18;193(12):1373–82.

2. Schaerli P, Willimann K, Lang AB, Lipp M, Loetscher P, Moser B. Cxc Chemokine Receptor 5 Expression Defines Follicular Homing T Cells with B Cell Helper Function. Journal of Experimental Medicine. 2000 Nov 27;192(11):1553–62.

3. Breitfeld D, Ohl L, Kremmer E, Ellwart J, Sallusto F, Lipp M, et al. Follicular B Helper T Cells Express Cxc Chemokine Receptor 5, Localize to B Cell Follicles, and Support Immunoglobulin Production. Journal of Experimental Medicine. 2000 Nov 27;192(11):1545–52.

4. Ballesteros-Tato A, León B, Graf BA, Moquin A, Adams PS, Lund FE, et al. Interleukin-2 Inhibits Germinal Center Formation by Limiting T Follicular Helper Cell Differentiation. Immunity. 2012 May 25;36(5):847–56.

5. Yu D, Rao S, Tsai LM, Lee SK, He Y, Sutcliffe EL, et al. The Transcriptional Repressor Bcl-6 Directs T Follicular Helper Cell Lineage Commitment. Immunity. 2009 Sep 18;31(3):457–68.

6. Nurieva RI, Chung Y, Martinez GJ, Yang XO, Tanaka S, Matskevitch TD, et al. Bcl6 Mediates the Development of T Follicular Helper Cells. Science. 2009 Aug 21;325(5943):1001–5.

7. Crotty S. T Follicular Helper Cell Differentiation, Function, and Roles in Disease. Immunity. 2014 Oct 16;41(4):529–42.

8. Cyster JG, Allen CDC. B Cell Responses: Cell Interaction Dynamics and Decisions. Cell. 2019 Apr 18;177(3):524–40.

9. Choi YS, Kageyama R, Eto D, Escobar TC, Johnston RJ, Monticelli L, et al. ICOS Receptor Instructs T Follicular Helper Cell versus Effector Cell Differentiation via Induction of the Transcriptional Repressor Bcl6. Immunity. 2011 Jun 24;34(6):932–46.

10. Liu D, Xu H, Shih C, Wan Z, Ma X, Ma W, et al. T–B-cell entanglement and ICOSL-driven feed-forward regulation of germinal centre reaction. Nature. 2015 Jan;517(7533):214–8.

11. Wen Y, Jing Y, Yang L, Kang D, Jiang P, Li N, et al. The regulators of BCR signaling during B cell activation. Blood Science. 2019 Oct;1(2):119–29.

12. Rawlings DJ, Schwartz MA, Jackson SW, Meyer-Bahlburg A. Integration of B cell responses through Toll-like receptors and antigen receptors. Nat Rev Immunol. 2012 Apr;12(4):282–94.

13. Martin F, Oliver AM, Kearney JF. Marginal Zone and B1 B Cells Unite in the Early Response against T-Independent Blood-Borne Particulate Antigens. Immunity. 2001 May 5;14(5):617–29.

14. Hua Z, Hou B. TLR signaling in B-cell development and activation. Cell Mol Immunol. 2013 Mar;10(2):103–6.

15. Elgueta R, Benson MJ, De Vries VC, Wasiuk A, Guo Y, Noelle RJ. Molecular mechanism and function of CD40/CD40L engagement in the immune system. Immunological Reviews. 2009;229(1):152–72.

16. Sasaki Y, Iwai K. Roles of the NF-κB Pathway in B-Lymphocyte Biology. In: Kurosaki T, Wienands J, editors. B Cell Receptor Signaling [Internet]. Cham: Springer International Publishing; 2016 [cited 2022 May 12]. p. 177–209. (Current Topics in Microbiology and Immunology). Available from: https://doi.org/10.1007/82_2015_479

17. Fruman DA, Limon JJ. Akt and mTOR in B Cell Activation and Differentiation. Front Immunol [Internet]. 2012 [cited 2021 Jan 23];3. Available from: https://www.frontiersin.org/articles/10.3389/fimmu.2012.00228/full#B70

18. Abdelrasoul H, Werner M, Setz CS, Okkenhaug K, Jumaa H. PI3K induces B-cell development and regulates B cell identity. Sci Rep. 2018 Jan 22;8(1):1327.

19. Thoreen CC, Chantranupong L, Keys HR, Wang T, Gray NS, Sabatini DM. A unifying model for mTORC1-mediated regulation of mRNA translation. Nature. 2012 May;485(7396):109–13.

20. Granato A, Hayashi EA, Baptista BJA, Bellio M, Nobrega A. IL-4 Regulates Bim Expression and Promotes B Cell Maturation in Synergy with BAFF Conferring Resistance to Cell Death at Negative Selection Checkpoints. The Journal of Immunology. 2014 Jun 15;192(12):5761–75.

21. Wurster AL, Rodgers VL, White MF, Rothstein TL, Grusby MJ. Interleukin-4-mediated Protection of Primary B Cells from Apoptosis through Stat6-dependent Up-regulation of Bcl-xL *. Journal of Biological Chemistry. 2002 Jul 26;277(30):27169–75.

22. Dufort FJ, Bleiman BF, Gumina MR, Blair D, Wagner DJ, Roberts MF, et al. Cutting Edge: IL-4-Mediated Protection of Primary B Lymphocytes from Apoptosis via Stat6-Dependent Regulation of Glycolytic Metabolism. The Journal of Immunology. 2007 Oct 15;179(8):4953–7.

23. Mehta DS, Wurster AL, Whitters MJ, Young DA, Collins M, Grusby MJ. IL-21 induces the apoptosis of resting and activated primary B cells. J Immunol. 2003 Apr 15;170(8):4111–8.

24. Kuchen S, Robbins R, Sims GP, Sheng C, Phillips TM, Lipsky PE, et al. Essential Role of IL-21 in B Cell Activation, Expansion, and Plasma Cell Generation during CD4+ T Cell-B Cell Collaboration. The Journal of Immunology. 2007 Nov 1;179(9):5886–96.

25. Vogelzang A, McGuire HM, Yu D, Sprent J, Mackay CR, King C. A Fundamental Role for Interleukin-21 in the Generation of T Follicular Helper Cells. Immunity. 2008 Jul 18;29(1):127–37.

26. Jacob J, Kelsoe G. In situ studies of the primary immune response to (4-hydroxy-3-nitrophenyl)acetyl. II. A common clonal origin for periarteriolar lymphoid sheath-associated foci and germinal centers. Journal of Experimental Medicine. 1992 Sep 1;176(3):679–87.

27. Taylor JJ, Pape KA, Jenkins MK. A germinal center–independent pathway generates unswitched memory B cells early in the primary response. Journal of Experimental Medicine. 2012 Feb 27;209(3):597–606.

28. Bannard O, Horton RM, Allen CDC, An J, Nagasawa T, Cyster JG. Germinal Center Centroblasts Transition to a Centrocyte Phenotype According to a Timed Program and Depend on the Dark Zone for Effective Selection. Immunity. 2013 Nov 14;39(5):912–24.

29. Allen CD, Okada T, Cyster JG. Germinal Center Organization and Cellular Dynamics. Immunity. 2007 Aug;27(2):190–202.

30. Allen CDC, Ansel KM, Low C, Lesley R, Tamamura H, Fujii N, et al. Germinal center dark and light zone organization is mediated by CXCR4 and CXCR5. Nat Immunol. 2004 Sep;5(9):943–52.

32. Caron G, Gallou SL, Lamy T, Tarte K, Fest T. CXCR4 Expression Functionally Discriminates Centroblasts versus Centrocytes within Human Germinal Center B Cells. The Journal of Immunology. 2009 Jun 15;182(12):7595–602.

33. Victora GD, Schwickert TA, Fooksman DR, Kamphorst AO, Meyer-Hermann M, Dustin ML, et al. Germinal Center Dynamics Revealed by Multiphoton Microscopy with a Photoactivatable Fluorescent Reporter. Cell. 2010 Nov 12;143(4):592–605.

34. Vinuesa CG, Linterman MA, Yu D, MacLennan ICM. Follicular Helper T Cells. Annual Review of Immunology. 2016;34(1):335–68.

35. Schroeder HW, Cavacini L. Structure and Function of Immunoglobulins. J Allergy Clin Immunol. 2010 Feb;125(2 0 2):S41–52.

36. Di Noia JM, Neuberger MS. Molecular Mechanisms of Antibody Somatic Hypermutation. Annual Review of Biochemistry. 2007;76(1):1–22.

37. Feng Y, Seija N, Noia JMD, Martin A. AID in Antibody Diversification: There and Back Again. Trends in Immunology. 2020 Jul 1;41(7):586–600.

38. Muramatsu M, Kinoshita K, Fagarasan S, Yamada S, Shinkai Y, Honjo T. Class switch recombination and hypermutation require activation-induced cytidine deaminase (AID), a potential RNA editing enzyme. Cell. 2000 Sep 1;102(5):553–63.

39. Xu Z, Zan H, Pone EJ, Mai T, Casali P. Immunoglobulin class-switch DNA recombination: induction, targeting and beyond. Nat Rev Immunol. 2012 Jul;12(7):517–31.

40. Kinoshita K, Honjo T. Linking class-switch recombination with somatic hypermutation. Nat Rev Mol Cell Biol. 2001 Jul;2(7):493–503.

41. Chi X, Li Y, Qiu X. V(D)J recombination, somatic hypermutation and class switch recombination of immunoglobulins: mechanism and regulation. Immunology. 2020;160(3):233–47.

42. Vaidyanathan B, Chaudhuri J. Epigenetic Codes Programing Class Switch Recombination. Front Immunol. 2015 Sep 11;6:405.

43. Wu H, Deng Y, Feng Y, Long D, Ma K, Wang X, et al. Epigenetic regulation in B-cell maturation and its dysregulation in autoimmunity. Cell Mol Immunol. 2018 Jul;15(7):676–84.

44. McBride KM, Gazumyan A, Woo EM, Barreto VM, Robbiani DF, Chait BT, et al. Regulation of hypermutation by activation-induced cytidine deaminase phosphorylation. Proceedings of the National Academy of Sciences. 2006 Jun 6;103(23):8798–803.

45. McBride KM, Gazumyan A, Woo EM, Schwickert TA, Chait BT, Nussenzweig MC. Regulation of class switch recombination and somatic mutation by AID phosphorylation. Journal of Experimental Medicine. 2008 Oct 6;205(11):2585–94.

46. Gazumyan A, Timachova K, Yuen G, Siden E, Di Virgilio M, Woo EM, et al. Amino-Terminal Phosphorylation of Activation-Induced Cytidine Deaminase Suppresses c-myc/IgH Translocation. Molecular and Cellular Biology. 2011 Feb;31(3):442–9.

47. Kitano M, Moriyama S, Ando Y, Hikida M, Mori Y, Kurosaki T, et al. Bcl6 Protein Expression Shapes Pre-Germinal Center B Cell Dynamics and Follicular Helper T Cell Heterogeneity. Immunity. 2011 Jun 24;34(6):961–72.

48. Cinamon G, Matloubian M, Lesneski MJ, Xu Y, Low C, Lu T, et al. Sphingosine 1-phosphate receptor 1 promotes B cell localization in the splenic marginal zone. Nat Immunol. 2004 Jul;5(7):713–20.

49. Green JA, Suzuki K, Cho B, Willison LD, Palmer D, Allen CDC, et al. The sphingosine 1-phosphate receptor S1P2 maintains the homeostasis of germinal center B cells and promotes niche confinement. Nat Immunol. 2011 Jul;12(7):672–80.

50. Huang C, Gonzalez DG, Cote CM, Jiang Y, Hatzi K, Teater M, et al. The BCL6 RD2 Domain Governs Commitment of Activated B Cells to Form Germinal Centers. Cell Reports. 2014 Sep 11;8(5):1497–508.

51. Phan RT, Dalla-Favera R. The BCL6 proto-oncogene suppresses p53 expression in germinal-centre B cells. Nature. 2004 Dec;432(7017):635–9.

52. Phan RT, Saito M, Basso K, Niu H, Dalla-Favera R. BCL6 interacts with the transcription factor Miz-1 to suppress the cyclin-dependent kinase inhibitor p21 and cell cycle arrest in germinal center B cells. Nat Immunol. 2005 Oct;6(10):1054–60.

53. Ranuncolo SM, Polo JM, Dierov J, Singer M, Kuo T, Greally J, et al. Bcl-6 mediates the germinal center B cell phenotype and lymphomagenesis through transcriptional repression of the DNA-damage sensor ATR. Nat Immunol. 2007 Jul;8(7):705–14.

54. Calado DP, Sasaki Y, Godinho SA, Pellerin A, Köchert K, Sleckman BP, et al. The cell-cycle regulator c-Myc is essential for the formation and maintenance of germinal centers. Nat Immunol. 2012 Nov;13(11):1092–100.

55. Finkin S, Hartweger H, Oliveira TY, Kara EE, Nussenzweig MC. Protein Amounts of the MYC Transcription Factor Determine Germinal Center B Cell Division Capacity. Immunity. 2019 Aug 20;51(2):324-336.e5.

56. Shapiro-Shelef M, Lin KI, McHeyzer-Williams LJ, Liao J, McHeyzer-Williams MG, Calame K. Blimp-1 Is Required for the Formation of Immunoglobulin Secreting Plasma Cells and Pre-Plasma Memory B Cells. Immunity. 2003 Oct 1;19(4):607–20.

57. Shaffer AL, Lin KI, Kuo TC, Yu X, Hurt EM, Rosenwald A, et al. Blimp-1 Orchestrates Plasma Cell Differentiation by Extinguishing the Mature B Cell Gene Expression Program. Immunity. 2002 Jul 1;17(1):51–62.

58. Shaffer AL, Shapiro-Shelef M, Iwakoshi NN, Lee AH, Qian SB, Zhao H, et al. XBP1, Downstream of Blimp-1, Expands the Secretory Apparatus and Other Organelles, and Increases Protein Synthesis in Plasma Cell Differentiation. Immunity. 2004 Jul 1;21(1):81–93.

59. Dominguez-Sola D, Kung J, Holmes AB, Wells VA, Mo T, Basso K, et al. The FOXO1 Transcription Factor Instructs the Germinal Center Dark Zone Program. Immunity. 2015 Dec 15;43(6):1064–74.

60. Sander S, Chu VT, Yasuda T, Franklin A, Graf R, Calado DP, et al. PI3 Kinase and FOXO1 Transcription Factor Activity Differentially Control B Cells in the Germinal Center Light and Dark Zones. Immunity. 2015 Dec 15;43(6):1075–86.

61. Tunyaplin C, Shaffer AL, Angelin-Duclos CD, Yu X, Staudt LM, Calame KL. Direct Repression of prdm1 by Bcl-6 Inhibits Plasmacytic Differentiation. The Journal of Immunology. 2004 Jul 15;173(2):1158–65.

62. Crotty S, Johnston RJ, Schoenberger SP. Effectors and memories: Bcl-6 and Blimp-1 in T and B lymphocyte differentiation. Nat Immunol. 2010 Feb;11(2):114–20.

63. Michalek RD, Gerriets VA, Jacobs SR, Macintyre AN, MacIver NJ, Mason EF, et al. Cutting Edge: Distinct Glycolytic and Lipid Oxidative Metabolic Programs

Are Essential for Effector and Regulatory CD4+ T Cell Subsets. The Journal of Immunology. 2011 Mar 15;186(6):3299–303.

64. Yang K, Blanco DB, Chen X, Dash P, Neale G, Rosencrance C, et al. Metabolic signaling directs the reciprocal lineage decisions of αβ and γδ T cells. Science Immunology. 2018 Jul 6;3(25):eaas9818.

65. Chi H. Regulation and function of mTOR signalling in T cell fate decisions. Nat Rev Immunol. 2012 May;12(5):325–38.

66. Krawczyk CM, Holowka T, Sun J, Blagih J, Amiel E, DeBerardinis RJ, et al. Toll-like receptor–induced changes in glycolytic metabolism regulate dendritic cell activation. Blood. 2010 Jun 10;115(23):4742–9.

67. Mills CD, Kincaid K, Alt JM, Heilman MJ, Hill AM. M-1/M-2 Macrophages and the Th1/Th2 Paradigm. The Journal of Immunology. 2000 Jun 15;164(12):6166–73.

68. Martinez FO, Helming L, Gordon S. Alternative Activation of Macrophages: An Immunologic Functional Perspective. Annual Review of Immunology. 2009;27(1):451–83.

69. Liu Y, Xu R, Gu H, Zhang E, Qu J, Cao W, et al. Metabolic reprogramming in macrophage responses. Biomarker Research. 2021 Jan 6;9(1):1.

70. Kelly B, O'Neill LA. Metabolic reprogramming in macrophages and dendritic cells in innate immunity. Cell Res. 2015 Jul;25(7):771–84.

71. Nagy C, Haschemi A. Time and Demand are Two Critical Dimensions of Immunometabolism: The Process of Macrophage Activation and the Pentose Phosphate Pathway. Front Immunol. 2015 Apr 8;6:164.

72. Baardman J, Verberk SGS, Prange KHM, van Weeghel M, van der Velden S, Ryan DG, et al. A Defective Pentose Phosphate Pathway Reduces Inflammatory Macrophage Responses during Hypercholesterolemia. Cell Rep. 2018 Nov 20;25(8):2044-2052.e5.

73. Haschemi A, Kosma P, Gille L, Evans CR, Burant CF, Starkl P, et al. The Sedoheptulose Kinase CARKL Directs Macrophage Polarization through Control of Glucose Metabolism. Cell Metabolism. 2012 Jun 6;15(6):813–26.

74. Tan Z, Xie N, Cui H, Moellering DR, Abraham E, Thannickal VJ, et al. Pyruvate Dehydrogenase Kinase 1 Participates in Macrophage Polarization via Regulating Glucose Metabolism. The Journal of Immunology. 2015 Jun 15;194(12):6082–9.

75. Huang SCC, Smith AM, Everts B, Colonna M, Pearce EL, Schilling JD, et al. Metabolic Reprogramming Mediated by the mTORC2-IRF4 Signaling Axis Is Essential for Macrophage Alternative Activation. Immunity. 2016 Oct 18;45(4):817–30.

76. Gergely P, Grossman C, Niland B, Puskas F, Neupane H, Allam F, et al. Mitochondrial hyperpolarization and ATP depletion in patients with systemic lupus erythematosus. Arthritis Rheum. 2002 Jan;46(1):175–90.

77. PERL A, GERGELY P, BANKI K. Mitochondrial Dysfunction in T Cells of Patients with Systemic Lupus Erythematosus. International Reviews of Immunology. 2004 Jan 1;23(3–4):293–313.

78. Morel L. Immunometabolism in systemic lupus erythematosus. Nat Rev Rheumatol. 2017 May;13(5):280–90.

79. Yin Y, Choi SC, Xu Z, Zeumer L, Kanda N, Croker BP, et al. Glucose Oxidation Is Critical for CD4+ T Cell Activation in a Mouse Model of Systemic Lupus Erythematosus. The Journal of Immunology. 2016 Jan 1;196(1):80–90.

80. Lui SL, Tsang R, Chan KW, Zhang F, Tam S, Yung S, et al. Rapamycin attenuates the severity of established nephritis in lupus-prone NZB/W F 1 mice. Nephrology Dialysis Transplantation. 2008 Sep 1;23(9):2768–76.

81. Sukhbaatar N, Hengstschläger M, Weichhart T. mTOR-Mediated Regulation of Dendritic Cell Differentiation and Function. Trends in Immunology. 2016 Nov 1;37(11):778–89.

82. Wang Y, Huang G, Zeng H, Yang K, Lamb RF, Chi H. Tuberous sclerosis 1 (Tsc1)-dependent metabolic checkpoint controls development of dendritic cells. Proc Natl Acad Sci U S A. 2013 Dec 10;110(50):E4894–903.

83. Caro-Maldonado A, Wang R, Nichols AG, Kuraoka M, Milasta S, Sun LD, et al. Metabolic Reprogramming is Required for Antibody Production That is Suppressed in Anergic but Exaggerated in Chronically BAFF-Exposed B cells. J Immunol. 2014 Apr 15;192(8):3626–36.

84. Jellusova J, Cato MH, Apgar JR, Ramezani-Rad P, Leung CR, Chen C, et al. Gsk3 is a metabolic checkpoint regulator in B cells. Nat Immunol. 2017 Mar;18(3):303–12.

85. Doughty CA, Bleiman BF, Wagner DJ, Dufort FJ, Mataraza JM, Roberts MF, et al. Antigen receptor–mediated changes in glucose metabolism in B lymphocytes: role of phosphatidylinositol 3-kinase signaling in the glycolytic control of growth. Blood. 2006 Jun 1;107(11):4458–65.

86. Maratou E, Dimitriadis G, Kollias A, Boutati E, Lambadiari V, Mitrou P, et al. Glucose transporter expression on the plasma membrane of resting and activated white blood cells. European Journal of Clinical Investigation. 2007;37(4):282–90.

87. Waters LR, Ahsan FM, Wolf DM, Shirihai O, Teitell MA. Initial B Cell Activation Induces Metabolic Reprogramming and Mitochondrial Remodeling. iScience. 2018 Jul 27;5:99–109.

88. Blair D, Dufort FJ, Chiles TC. Protein kinase Cβ is critical for the metabolic switch to glycolysis following B-cell antigen receptor engagement. Biochemical Journal. 2012 Oct 18;448(1):165–9.

89. Tsui C, Martinez-Martin N, Gaya M, Maldonado P, Llorian M, Legrave NM, et al. Protein Kinase C-β Dictates B Cell Fate by Regulating Mitochondrial Remodeling, Metabolic Reprogramming, and Heme Biosynthesis. Immunity. 2018 Jun 19;48(6):1144-1159.e5.

90. Dufort FJ, Gumina MR, Ta NL, Tao Y, Heyse SA, Scott DA, et al. Glucose-dependent de Novo Lipogenesis in B Lymphocytes. J Biol Chem. 2014 Mar 7;289(10):7011–24.

91. Akkaya M, Traba J, Roesler AS, Miozzo P, Akkaya B, Theall BP, et al. Second signals rescue B cells from activation-induced mitochondrial dysfunction and death. Nat Immunol. 2018 Aug;19(8):871–84.

92. Caldwell RG, Wilson JB, Anderson SJ, Longnecker R. Epstein-Barr Virus LMP2A Drives B Cell Development and Survival in the Absence of Normal B Cell Receptor Signals. Immunity. 1998 Sep 1;9(3):405–11.

93. Mancao C, Hammerschmidt W. Epstein-Barr virus latent membrane protein 2A is a B-cell receptor mimic and essential for B-cell survival. Blood. 2007 Nov 15;110(10):3715–21.

94. Miller CL, Lee JH, Kieff E, Longnecker R. An integral membrane protein (LMP2) blocks reactivation of Epstein-Barr virus from latency following surface immunoglobulin crosslinking. Proceedings of the National Academy of Sciences. 1994 Jan 18;91(2):772–6.

95. Portis T, Longnecker R. Epstein–Barr virus (EBV) LMP2A mediates B-lymphocyte survival through constitutive activation of the Ras/PI3K/Akt pathway. Oncogene. 2004 Nov;23(53):8619–28.

96. Swart R, Ruf IK, Sample J, Longnecker R. Latent Membrane Protein 2A-Mediated Effects on the Phosphatidylinositol 3-Kinase/Akt Pathway. Journal of Virology. 2000 Nov 15;74(22):10838–45.

97. Fruehling S, Longnecker R. The Immunoreceptor Tyrosine-Based Activation Motif of Epstein–Barr Virus LMP2A Is Essential for Blocking BCR-Mediated Signal Transduction. Virology. 1997 Sep 1;235(2):241–51.

98. Fish K, Comoglio F, Shaffer AL, Ji Y, Pan KT, Scheich S, et al. Rewiring of B cell receptor signaling by Epstein–Barr virus LMP2A. Proceedings of the National Academy of Sciences. 2020 Oct 20;117(42):26318–27.

99. Wang LW, Shen H, Nobre L, Ersing I, Paulo JA, Trudeau S, et al. Epstein-Barr-Virus-Induced One-Carbon Metabolism Drives B Cell Transformation. Cell Metabolism. 2019 Sep 3;30(3):539-555.e11.

100. Furukawa K, Tengler R, Nakamura M, Urwyler A, De Weck AL, Kanegasaki S, et al. B Lymphoblasts show Oxidase Activity in Response to Cross-Linking of

Surface IgM and HLA-DR. Scandinavian Journal of Immunology. 1992;35(5):561–7.

101. Wheeler ML, DeFranco AL. Prolonged Production of Reactive Oxygen Species in Response to B Cell Receptor Stimulation Promotes B Cell Activation and Proliferation. The Journal of Immunology. 2012 Nov 1;189(9):4405–16.

102. Bertolotti M, Yim SH, Garcia-Manteiga JM, Masciarelli S, Kim YJ, Kang MH, et al. B- to Plasma-Cell Terminal Differentiation Entails Oxidative Stress and Profound Reshaping of the Antioxidant Responses. Antioxidants & Redox Signaling. 2010 Oct 15;13(8):1133–44.

103. Jang KJ, Mano H, Aoki K, Hayashi T, Muto A, Nambu Y, et al. Mitochondrial function provides instructive signals for activation-induced B-cell fates. Nat Commun. 2015 Apr 10;6(1):6750.

104. Laidlaw BJ, Cyster JG. Transcriptional regulation of memory B cell differentiation. Nat Rev Immunol. 2021 Apr;21(4):209–20.

105. Lin WHW, Adams WC, Nish SA, Chen YH, Yen B, Rothman NJ, et al. Asymmetric PI3K Signaling Driving Developmental and Regenerative Cell Fate Bifurcation. Cell Rep. 2015 Dec 15;13(10):2203–18.

106. Ochiai K, Maienschein-Cline M, Simonetti G, Chen J, Rosenthal R, Brink R, et al. Transcriptional regulation of germinal center B and plasma cell fates by dynamical control of IRF4. Immunity. 2013 May 23;38(5):918–29.

107. Sciammas R, Shaffer AL, Schatz JH, Zhao H, Staudt LM, Singh H. Graded expression of interferon regulatory factor-4 coordinates isotype switching with plasma cell differentiation. Immunity. 2006 Aug;25(2):225–36.

108. Calnan DR, Brunet A. The FoxO code. Oncogene. 2008 Apr;27(16):2276–88.

109. Price MJ, Patterson DG, Scharer CD, Boss JM. Progressive Upregulation of Oxidative Metabolism Facilitates Plasmablast Differentiation to a T-Independent Antigen. Cell Reports. 2018 Jun 12;23(11):3152–9.

110. Lam WY, Becker AM, Kennerly KM, Wong R, Curtis JD, Llufrio EM, et al. Mitochondrial Pyruvate Import Promotes Long-Term Survival of Antibody-Secreting Plasma Cells. Immunity. 2016 Jul 19;45(1):60–73.

111. Jayachandran N, Mejia EM, Sheikholeslami K, Sher AA, Hou S, Hatch GM, et al. TAPP Adaptors Control B Cell Metabolism by Modulating the Phosphatidylinositol 3-Kinase Signaling Pathway: A Novel Regulatory Circuit Preventing Autoimmunity. The Journal of Immunology. 2018 Jul 15;201(2):406–16.

112. Weisel FJ, Mullett SJ, Elsner RA, Menk AV, Trivedi N, Luo W, et al. Germinal center B cells selectively oxidize fatty acids for energy while conducting minimal glycolysis. Nat Immunol. 2020 Mar;21(3):331–42.

113. Inoue T, Shinnakasu R, Kawai C, Ise W, Kawakami E, Sax N, et al. Exit from germinal center to become quiescent memory B cells depends on metabolic reprograming and provision of a survival signal. Journal of Experimental Medicine. 2020 Oct 12;218(1):e20200866.

114. Ersching J, Efeyan A, Mesin L, Jacobsen JT, Pasqual G, Grabiner BC, et al. Germinal Center Selection and Affinity Maturation Require Dynamic Regulation of mTORC1 Kinase. Immunity. 2017 Jun 20;46(6):1045-1058.e6.

115. Goetzman ES, Prochownik EV. The Role for Myc in Coordinating Glycolysis, Oxidative Phosphorylation, Glutaminolysis, and Fatty Acid Metabolism in Normal and Neoplastic Tissues. Frontiers in Endocrinology [Internet]. 2018 [cited 2022 Apr 8];9. Available from: https://www.frontiersin.org/article/10.3389/fendo.2018.00129

116. Luo W, Weisel F, Shlomchik MJ. B Cell Receptor and CD40 Signaling Are Rewired for Synergistic Induction of the c-Myc Transcription Factor in Germinal Center B Cells. Immunity. 2018 Feb 20;48(2):313-326.e5.

117. McGettrick AF, O'Neill LAJ. The Role of HIF in Immunity and Inflammation. Cell Metab. 2020 Oct 6;32(4):524–36.

118. Cho SH, Raybuck AL, Stengel K, Wei M, Beck TC, Volanakis E, et al. Germinal centre hypoxia and regulation of antibody qualities by a hypoxia response system. Nature. 2016 Sep;537(7619):234–8.

119. Ducker GS, Rabinowitz JD. One-Carbon Metabolism in Health and Disease. Cell Metabolism. 2017 Jan;25(1):27–42.

120. Yang M, Vousden KH. Serine and one-carbon metabolism in cancer. Nat Rev Cancer. 2016 Oct;16(10):650–62.

121. Amelio I, Cutruzzolá F, Antonov A, Agostini M, Melino G. Serine and glycine metabolism in cancer. Trends in Biochemical Sciences. 2014 Apr;39(4):191.

122. Chaneton B, Hillmann P, Zheng L, Martin ACL, Maddocks ODK, Chokkathukalam A, et al. Serine is a natural ligand and allosteric activator of pyruvate kinase M2. Nature. 2012 Nov;491(7424):458–62.

123. Pakos-Zebrucka K, Koryga I, Mnich K, Ljujic M, Samali A, Gorman AM. The integrated stress response. EMBO Rep. 2016 Oct;17(10):1374–95.

124. Wek RC. Role of eIF2α Kinases in Translational Control and Adaptation to Cellular Stress. Cold Spring Harb Perspect Biol. 2018 Jan 7;10(7):a032870.

125. Ye J, Mancuso A, Tong X, Ward PS, Fan J, Rabinowitz JD, et al. Pyruvate kinase M2 promotes de novo serine synthesis to sustain mTORC1 activity and cell proliferation. PNAS. 2012 May 1;109(18):6904–9.

126. Ducker GS, Chen L, Morscher RJ, Ghergurovich JM, Esposito M, Teng X, et al. Reversal of Cytosolic One-Carbon Flux Compensates for Loss of the Mitochondrial Folate Pathway. Cell Metabolism. 2016 Jun 14;23(6):1140–53.

127. Zheng Y, Cantley LC. Toward a better understanding of folate metabolism in health and disease. J Exp Med. 2019 Feb 4;216(2):253–66.

128. Struck AW, Thompson ML, Wong LS, Micklefield J. S-Adenosyl-Methionine-Dependent Methyltransferases: Highly Versatile Enzymes in Biocatalysis, Biosynthesis and Other Biotechnological Applications. ChemBioChem. 2012;13(18):2642–55.

129. Jain M, Nilsson R, Sharma S, Madhusudhan N, Kitami T, Souza AL, et al. Metabolite Profiling Identifies a Key Role for Glycine in Rapid Cancer Cell Proliferation. Science. 2012 May 25;336(6084):1040–4.

130. Maddocks ODK, Berkers CR, Mason SM, Zheng L, Blyth K, Gottlieb E, et al. Serine starvation induces stress and p53-dependent metabolic remodelling in cancer cells. Nature. 2013 Jan;493(7433):542–6.

131. Labuschagne CF, van den Broek NJF, Mackay GM, Vousden KH, Maddocks ODK. Serine, but Not Glycine, Supports One-Carbon Metabolism and Proliferation of Cancer Cells. Cell Reports. 2014 May 22;7(4):1248–58.

132. DeNicola GM, Chen PH, Mullarky E, Sudderth JA, Hu Z, Wu D, et al. NRF2 regulates serine biosynthesis in non–small cell lung cancer. Nat Genet. 2015 Dec;47(12):1475–81.

133. Anastasiou D, Poulogiannis G, Asara JM, Boxer MB, Jiang J kang, Shen M, et al. Inhibition of Pyruvate Kinase M2 by Reactive Oxygen Species Contributes to Cellular Antioxidant Responses. Science. 2011 Dec 2;334(6060):1278–83.

134. Sun L, Song L, Wan Q, Wu G, Li X, Wang Y, et al. cMyc-mediated activation of serine biosynthesis pathway is critical for cancer progression under nutrient deprivation conditions. Cell Res. 2015 Apr;25(4):429–44.

135. Mitsuishi Y, Taguchi K, Kawatani Y, Shibata T, Nukiwa T, Aburatani H, et al. Nrf2 Redirects Glucose and Glutamine into Anabolic Pathways in Metabolic Reprogramming. Cancer Cell. 2012 Jul 10;22(1):66–79.

136. Ding J, Li T, Wang X, Zhao E, Choi JH, Yang L, et al. The Histone H3 Methyltransferase G9A Epigenetically Activates the Serine-Glycine Synthesis Pathway to Sustain Cancer Cell Survival and Proliferation. Cell Metabolism. 2013 Dec 3;18(6):896–907.

137. Zhao E, Ding J, Xia Y, Liu M, Ye B, Choi JH, et al. KDM4C and ATF4 Cooperate in Transcriptional Control of Amino Acid Metabolism. Cell Reports. 2016 Jan 26;14(3):506–19.

138. Berry WL, Janknecht R. KDM4/JMJD2 Histone Demethylases: Epigenetic Regulators in Cancer Cells. Cancer Research. 2013 May 12;73(10):2936–42.

139. Lee GY, Haverty PM, Li L, Kljavin NM, Bourgon R, Lee J, et al. Comparative Oncogenomics Identifies PSMB4 and SHMT2 as Potential Cancer Driver Genes. Cancer Research. 2014 May 29;74(11):3114–26.

140. Ma EH, Bantug G, Griss T, Condotta S, Johnson RM, Samborska B, et al. Serine Is an Essential Metabolite for Effector T Cell Expansion. Cell Metabolism. 2017 Feb 7;25(2):345–57.

141. Ron-Harel N, Santos D, Ghergurovich JM, Sage PT, Reddy A, Lovitch SB, et al. Mitochondrial Biogenesis and Proteome Remodeling Promote One-Carbon Metabolism for T Cell Activation. Cell Metab. 2016 Jul 12;24(1):104–17.

142. Ron-Harel N, Notarangelo G, Ghergurovich JM, Paulo JA, Sage PT, Santos D, et al. Defective respiration and one-carbon metabolism contribute to impaired naïve T cell activation in aged mice. Proceedings of the National Academy of Sciences. 2018 Dec 26;115(52):13347–52.

143. Rodriguez AE, Ducker GS, Billingham LK, Martinez CA, Mainolfi N, Suri V, et al. Serine Metabolism Supports Macrophage IL-1β Production. Cell Metabolism. 2019 Apr 2;29(4):1003-1011.e4.

144. Yu W, Wang Z, Zhang K, Chi Z, Xu T, Jiang D, et al. One-Carbon Metabolism Supports S-Adenosylmethionine and Histone Methylation to Drive Inflammatory Macrophages. Molecular Cell. 2019 Sep 19;75(6):1147-1160.e5.

145. Kurita K, Ohta H, Shirakawa I, Tanaka M, Kitaura Y, Iwasaki Y, et al. Macrophages rely on extracellular serine to suppress aberrant cytokine production. Sci Rep. 2021 May 27;11(1):11137.

146. D'Avola A, Legrave N, Tajan M, Chakravarty P, Shearer RL, King HW, et al. PHGDH is required for germinal center formation and is a therapeutic target in *MYC*-driven lymphoma. J Clin Invest [Internet]. 2022 May 2 [cited 2022 May 11];132(9). Available from: https://www.jci.org/articles/view/153436#F3

147. Hobeika E, Thiemann S, Storch B, Jumaa H, Nielsen PJ, Pelanda R, et al. Testing gene function early in the B cell lineage in mb1-cre mice. Proceedings of the National Academy of Sciences. 2006 Sep 12;103(37):13789–94.

148. Yoshida K, Furuya S, Osuka S, Mitoma J, Shinoda Y, Watanabe M, et al. Targeted Disruption of the Mouse 3-Phosphoglycerate Dehydrogenase Gene Causes Severe Neurodevelopmental Defects and Results in Embryonic Lethality*. Journal of Biological Chemistry. 2004 Jan 30;279(5):3573–7.

149. Pacold ME, Brimacombe KR, Chan SH, Rohde JM, Lewis CA, Swier LJYM, et al. A PHGDH inhibitor reveals coordination of serine synthesis and one-carbon unit fate. Nat Chem Biol. 2016 Jun;12(6):452–8.

150. Zaheen A, Martin A. Induction and Assessment of Class Switch Recombination in Purified Murine B Cells. J Vis Exp. 2010 Aug 13;(42):2130.

151. Zan H, Casali P. Epigenetics of Peripheral B-Cell Differentiation and the Antibody Response. Front Immunol. 2015 Dec 14;6:631.

152. Battu S, Minhas G, Mishra A, Khan N. Amino Acid Sensing via General Control Nonderepressible-2 Kinase and Immunological Programming. Front Immunol

[Internet]. 2017 [cited 2021 Jan 23];8. Available from: https://www.frontiersin.org/articles/10.3389/fimmu.2017.01719/full

153. Lee F, Yokota T, Otsuka T, Meyerson P, Villaret D, Coffman R, et al. Isolation and characterization of a mouse interleukin cDNA clone that expresses B-cell stimulatory factor 1 activities and T-cell- and mast-cell-stimulating activities. Proc Natl Acad Sci U S A. 1986 Apr;83(7):2061–5.

154. Hay N, Sonenberg N. Upstream and downstream of mTOR. Genes Dev. 2004 Aug 15;18(16):1926–45.

155. Maddocks ODK, Athineos D, Cheung EC, Lee P, Zhang T, van den Broek NJF, et al. Modulating the therapeutic response of tumours to dietary serine and glycine starvation. Nature. 2017 Apr;544(7650):372–6.

156. Ngo B, Kim E, Osorio-Vasquez V, Doll S, Bustraan S, Liang RJ, et al. Limited Environmental Serine and Glycine Confer Brain Metastasis Sensitivity to PHGDH Inhibition. Cancer Discovery. 2020 Sep 1;10(9):1352–73.